Index

1. Introduction -4-

1.1 Myocardial Infarction -4-

1.2 Ischemic Neovascularization and Angiogenesis -4-

1.3 Stem Cells -6-

1.3.1 Mesenchymal Stem or Stromal Cells -7-

1.4 Nitric Oxide -7-

1.5 The IGF-1 Protein -10-

1.6 Aim of the Study -13-

2. Materials and Methods -14-

2.1 Isolation of adipose derived MSC -14-

2.1.1 Materials -14-

2.1.2 Method -14-

2.2 Culture of MSC -15-

2.2.1 Materials -15-

2.2.2 Method -15-

2.3 Synthesis of the Active Site of IGF-1 Linked to NapFFG -16-

2.3.1 Materials -16-

2.3.2 Method -17-

2.4 Preparation of the Hydrogel -19-

2.4.1 Materials -19-

2.4.2 Method -19-

2.5 *In Vitro* Studies -20-

2.5.1 MTT Cell Proliferation Assay -20-

2.5.1.1 Materials -20-

2.5.1.2 Method -20-

2.5.2 Reverse Transcription-qPCR -21-

2.5.2.1 Materials -21-

2.5.2.2 Method -22-

2.6 *In vivo* Studies -23-

2.6.1 C57 Cell Labeling -23-

2.6.1.1 Materials -23-
2.6.1.2 Method -24-
2.6.2 Animal Surgery -24-
2.6.2.1 Materials -24-
2.6.2.2 Method -25-
2.6.3 Molecular Imaging and Cell Tracking in Living Animals -26-
2.6.3.1 Materials -26-
2.6.3.2 Method -26-
2.6.4 Collection of the Infarcted Heart -26-
2.6.4.1 Materials -26-
2.6.4.2 Method -27-
2.6.5 Histological Analysis -27-
2.6.5.1 Materials -27-
2.6.5.2 Method -27-
2.6.5.2.1 HE Staining -28-
2.6.5.2.1.1 Materials -28-
2.6.5.2.1.2 Method -28-
2.6.5.2.2 Masson's Trichrome Staining -28-
2.6.5.2.2.1 Materials -28-
2.6.5.2.2.2 Method -29-
2.7 Statistical Analysis -29-
3. Results -30-
3.1 Analysis of NapFFG-IGF-1 Peptide by LC-MS -30-
3.2 Proliferative Effects of Nitric Oxide and the Active Site of IGF-1 - Hydrogel on MSC -31-
3.3 Angiogenic Potential of the Nitric Oxide Releasing Hydrogel and of the IGF-1-active Site Hydrogel -32-
3.4 Anti-inflammatory Potential of a Nitric Oxide Releasing Hydrogel and the IGF-1-active Site Hydrogel -35-
3.5 Effects of a Nitric Oxide-Releasing-Hydrogel on Cell Survival in a Mouse Model -38-
3.6 Impact of a Nitric Oxide-releasing-hydrogel on the Infarct Size in a Mouse -42-

Model
4. Discussion -48-
5. Conclusion and Future Perspectives -53-
6. References -54-
7. Abbreviations -64-
8. Index of Figures -66-
9. Index of Tables -71-
10. Acknowledgements -72-
11. Declaration -73-

1. Introduction

1.1 Myocardial Infarction

Ischemic vascular diseases are the leading cause of death worldwide [1]. Myocardial infarction is defined by the presence of myocardial ischemia and death of cardiomyocytes and vascular structures due to ischemia after arterial occlusion. This results in cardiac remodeling including hypertrophy and apoptosis as well as in upregulation of inflammatory cytokines in the infarcted heart [2-5]. Necrosis of cardiomyocytes leads to fibrous scar formation that causes a non-reversible loss of the rhythmic contractile abilities and heart function [6-9]. Therefore, the instauration of the blood flow to the ischemic tissue is necessary to prevent tissue death after arterial occlusion [1][5]. However, ischemia driven angiogenesis is insufficient to avoid further impairment of the ischemic heart. For this reason research has recently focused on angiogenesis inducing models after myocardial infarction [8][10-11].

1.2 Ischemic Neovascularization and Angiogenesis

Ischemic neovascularization involves three major processes: angiogenesis, arteriogenesis and post-natal vasculogenesis. These processes are driven by several cellular and molecular pathways. These involve various angiogenic growth factors such as vascular endothelial growth factor (VEGF), fibroblast growth factor (FGF), platelet derived growth factor (PDGF) and signaling molecules, e.g. nitric oxide (NO), or transcription factors such as hypoxia-inducible factor-1 (HIF-1) or heat shock factor 1 (HSF-1) [1][10][12-15]. Additionally, also mechanical stimuli such as laminar shear stress and wall tension stretch stress regulate cell adhesion molecules and mitogenic factors which are stimulating these processes [1].

Angiogenesis is characterized by the formation of new capillaries from already existing blood vessels. The existing vessels are remodeled by sprouting and microvascular growth. The process starts with degradation of the basement membrane (BM) and the surrounding extracellular matrix (ECM), which leads to cell-matrix mediated outgrowth

of cells and tube formation. By the synthesis of BM proteins a new BM can be formed and is stabilized by pericytes. This process is primarily triggered by tissue hypoxia under ischemic conditions and is initiated by the activation of endothelial cells, which results in proliferation, migration and tube formation [1][12-13][16]. Moreover, this process is highly regulated by pro- and anti-angiogenic growth factors and their corresponding receptors. The local release of cytokines, chemokines and growth factors redirect circulating cells to the ischemic tissue. These growth factors, e.g. VEGF, are specific for the endothelium, while matrix metalloproteinases (MMPs) affect many different cells [17-19]. The most potent pro-angiogenic factor represents VEGF. Its expression is stimulated and regulated by several factors, including HIF-1 and can be inhibited by tumor necrosis factor alpha (TNFα). VEGF gradients guide the sprouting vessels while PDGF recruits pericytes [12][19-20]. VEGF is usually produced by endothelial cells, podocytes, macrophages, fibroblasts and by tumor cells or the adjacent stroma. It binds two tyrosine kinase receptors: VEGF receptor 1 (VEGFR-1) and VEGF receptor 2 (VEGFR-2). However, most of the VEGF signaling is mediated by VEGFR-2 which influences the mobilization of endothelial progenitor cells from the bone marrow, endothelial cell proliferation, migration, survival, tube formation and thereby enhances permeability [14][19]. These activities of VEGF operate via several pathways, including activation of the PI3 K/Akt (protein kinase B)/ mTOR pathway or activation of phospholipase C-γ (PLC-γ), protein kinase C (PKC), Raf-1, extracellular-signal-regulated protein kinase (ERK1/2), focal adhesion kinase (FAK) and mitogen activated protein kinase (MEK1/2) pathways. Furthermore, it induces vasodilation by the activation of the nitric oxide pathway. The VEGF signaling, influencing proliferation, survival, permeability responses and endothelial differentiation, occurs in a paracrine way while the survival of blood vessels is regulated through an autocrine signaling loop [19].

However, the basic fibroblast growth factor (bFGF) activates downstream MAPK signaling and triggers cell proliferation. Additionally, fibronectin stimulates endothelial cell survival as well as cell migration and increases VEGF activity. TGF-β has pro- and anti-angiogenic effects: At low doses it up-regulates the expression of angiogenic factors and ECM degrading proteases while high levels inhibit the endothelial cell growth and promote the reorganization of the BM [12][14]. After tube formation is

completed, the blood flow to the newly vascularized area raises local oxygen levels, thus, resulting in a decrease of VEGF levels which indicates the end of the angiogenic cycle (Fig.1) [12].

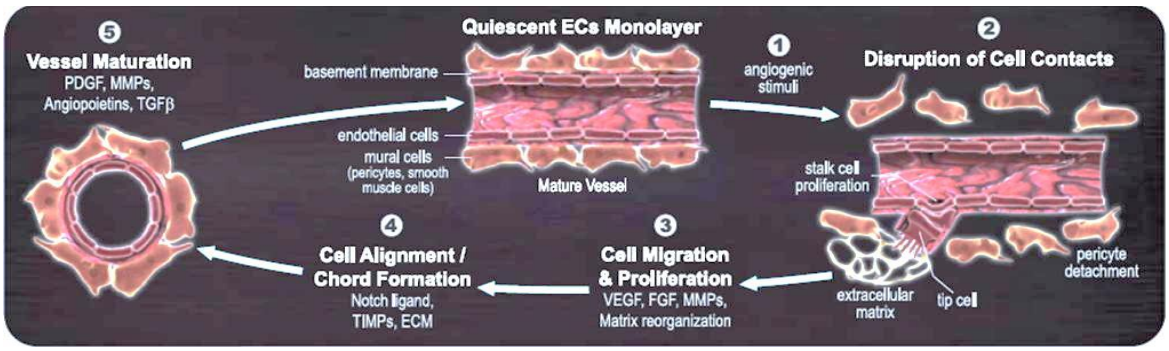

Fig.1: Process of angiogenesis in ischemic tissue [12]. For description see text.

In contrast to the ischemia-driven angiogenesis, hypoxia is not required for arteriogenesis. This process occurs under normoxic environments, far from ischemic tissue regions. Arteriogenesis includes the outward growth and remodeling of existing arterioles into larger arteries when a main artery is obstructed. Additionally to various factors, mechanical forces trigger this process. These processes are essential for regulating tissue neovascularization to restore blood perfusion to the ischemic region [1].

Mesenchymal stroma / stem cells (MSC) have the ability to secret soluble factors, such as VEGF, to induce angiogenesis in ischemic tissues, thus, influencing this complex process [10][21].

1.3 Stem Cells

In general, stem cells are described by their ability of self-renewal resulting in two identical stem cells and multi-lineage developmental/differentiation potential. Depending on their origin, they are characterized as embryonic stem cells with unlimited self-renewing capacity or as adult pluripotent stem cells [22]. Despite the totipotency of embryonic stem cells, their use in tissue regeneration is limited due to the dysregulated cell growth and teratoma formation [7][23].

1.3.1 Mesenchymal Stem or Stromal Cells

Mesenchymal stem or stromal cells (MSC) are adult pluripotent non-hematopoetic cells that are capable of self-renewal and differentiation into mesoderm-type cells [24-26]. MSC can be isolated from several adult tissues such as the bone marrow, adipose tissue, skin, blood, placenta and umbilical cord, brain, kidney, lung, teeth, pancreas and liver [7][24-25][27-28]. These cells are characterized by the lack of CD45, CD34, CD31, CD14 and CD11b and HLA-DR surface molecules but stain positive for the expression of CD29, CD44, CD73, CD105, CD106 and CD166 and show spindle-shaped fibroblast-like appearance in vitro [7][27-28].

Although adult stem cells exhibit a limited capability of differentiation, MSCs are known to differentiate into mesoderm-type cells like osteoblasts, chondrocytes and adipocytes as well as into a myogenic phenotype [7][24][26-28]. They were also shown to differentiate into smooth muscle and endothelial cell lineages and even cardiac-like myocytes [29-30]. In addition, MSCs release cytokines and growth factors which play an important role in cell survival and angiogenesis in both an autocrine and paracrine way. MSC secrete angiogenic cytokines such as VEGF, bFGF, angiopoietin-1, EPO, IGF-1 and MCP-1 [25][28-29][31]. Furthermore, MSCs also exert immune-modulatory effects and show no immune response after allogenic transplantation because of a lack of HLA-DR on their cell surface. This can be shown in undifferentiated and differentiated MSCs [7]. Therefore, MSC can be used for transplantation to influence immune modulation, tissue repair, and tissue regeneration after myocardial infarction [24][26-27].

1.4 Nitric Oxide

Nitric oxide (NO) is a diffusible free radical that functions as a pluripotent intracellular messenger and is highly diffusible in water and through biological membranes. It is an unstable gasotransmitter, which has a short half-life of seconds, influenced by the presence of oxygen-derived free radicals [1][32-33].

Nitric oxide synthase (NOS) is expressed as neuronal NOS, endotoxin- and cytokine-inducible NOS and endothelial NOS (eNOS) [32]. Endothelium derived NO was first identified as an endothelium derived relaxing factor. It triggers muscle relaxation in blood vessels and stimulates endothelial cell proliferation, migration, and pericyte recruitement as an angiogenic response in pathophysiological processes. Additionally, it inhibits platelet aggregation and leukocyte adherence to the endothelium [1][15][33-35].

The NO-system can be activated PKA-dependently, stimulating arteriogenesis and angiogenesis to restore the blood flow in ischemic tissue (Fig.2) or VEGF-dependently. VEGF binding on VEGFR2 stimulates the Akt/PKA-mediated NO production. This leads to increased cGMP formation and PKG activity as well as Ras, Raf and ERK1/2 signaling to effect angiogenesis via regulation of the EC proliferation and migration. Finally, cAMP/PKA signaling can activate PI3K/Akt to inhibit endothelial apoptosis and to enhance proliferation. The PKA/eNOS pathway induces endothelial migration via NO production and calcium influx. Furthermore, it promotes endothelial wound healing through cytoskeletal reorganization of focal adhesions [1]. NO is also known to stimulate angiogenesis through inducing the expression of ETS-1 [36].

Nitric oxide enhances the EC migration by stimulating EC podokines and by increasing bFGF-mediated dissolution of the extracellular matrix. The growth-promoting effect of NO is associated with cGMP generation in the endothelium. This increases VEGF and bFGF expression under physiologic conditions (in the vessel wall) as well as under pathologic conditions (inflammatory diseases) [1][34]. In contrast, NO at high concentrations reacts directly with oxygen resulting in nitration, nitrosation or nitrosylation. Therefore, excessive NO concentrations are known to be toxic. The cytotoxicity is related to the inhibition of complex 1 of the mitochondrial respiratory chain by S-nitrosation. This leads to a decreased electron flux through the respiratory chain and a decrease in ROS generation [32][35].

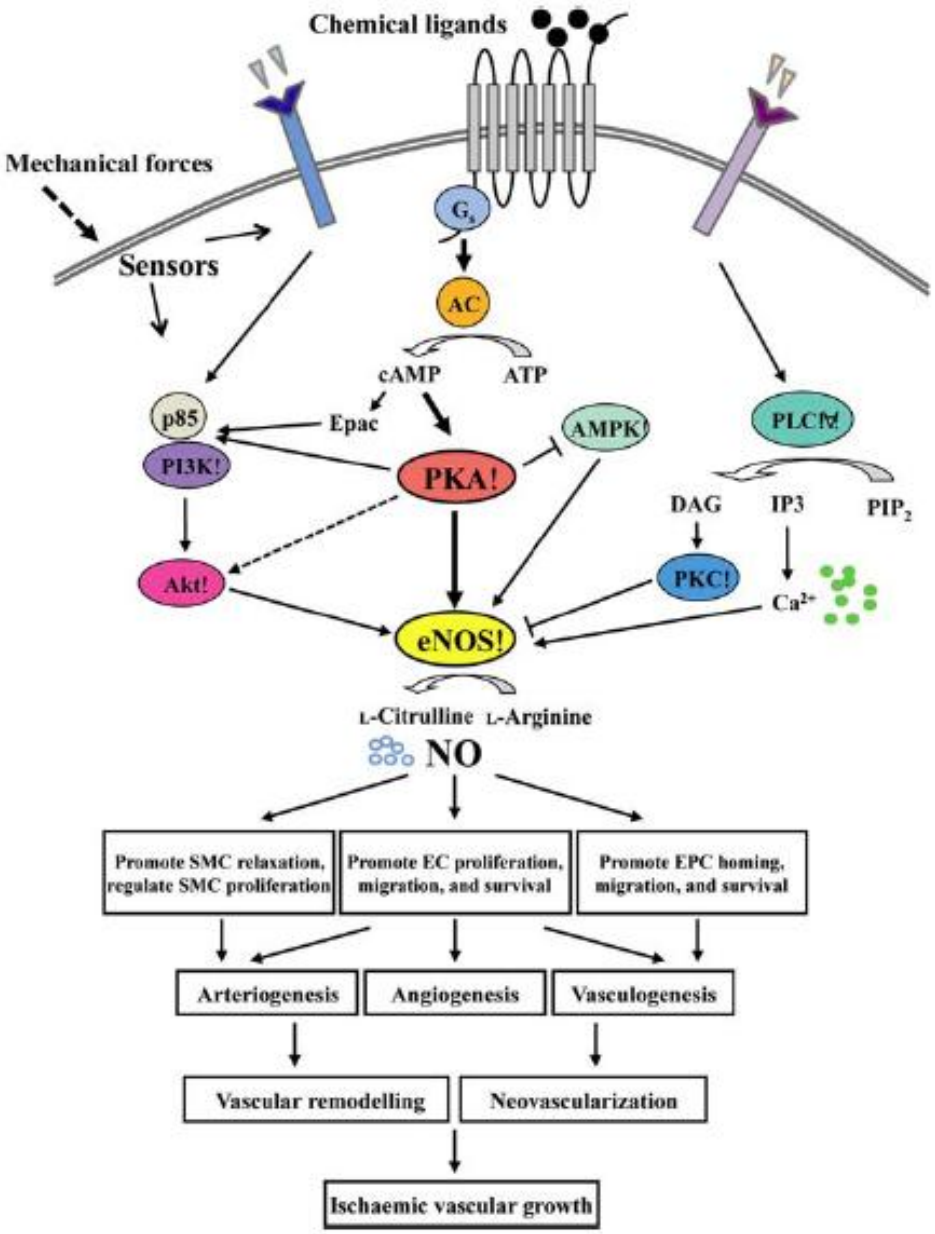

Fig.2: PKA signaling modulates the effects of NO in vascularization. PKA-dependent signaling pathway is activated by stimuli such as mechanical forces and chemical ligands which are regulating vessel growth. The PKA pathway interacts with several intracellular pathways (PI3K, Akt and AMPK) to activate eNOS/NO. eNOS/NO induces multiple cellular functions (cell proliferation, migration and survival) leading to angiogenesis and ischemic vessel growth [1].

High concentrations of NO in the heart and cardiovascular system trigger inflammation and suppress contractile function whereas NO at low concentrations increases the ventricular function [37]. Moreover, NO regulates cardiac contraction, oxygen

consumption, substrate utilization, apoptosis and hypertrophy. It may protect the heart by improving coronary vascular perfusion and contractile function, decreasing monocyte infiltration, reducing [Ca2+]m, damping respiration or inhibiting the mitochondrial pathway of apoptosis [32]. NO has been shown to play a key role in the regulation of cardiac hypertrophy and fibrosis in response to myocardial ischemia after infarction [3]. But the effect of a synthetic NO-donor with controlled NO release on mesenchymal stem / stroma cells in a transplantation study after myocardial infarction has not been investigated so far.

1.5 The IGF-1 Protein

Insulin like growth factor (IGF) proteins are growth hormones that stimulate the growth of tissues and cells. The IGF signaling mediates many critical cell responses including mitogenesis, proliferation, growth, differentiation and angiogenesis [20][38][39].

IGF-1 is a peptide hormone that is structurally related to insulin. It consist of a single chain of 70 amino acids, cross linked by three disulfide bridges and classified into four domains (A, B, C, D). The homology with insulin is specified by a 48% amino acid identity in the A and B domains as well as identical disulfide bonding and a similar tertiary structure [14][38][40].

IGF-1 binds with high affinity to the IGF-1-receptor (IGF1R) which is related to the insulin receptor (IR). IR and IGF1R show a high homology of 84% in the tyrosine kinase domain and 45%–65% homology in the ligand binding domain. Additionally, both receptors consist of two half-receptors that can randomly form hybrids, when an insulin half-receptor associates with an IGF half-receptor. The IGF1R is a tyrosine kinase receptor composed of a tetramer with two α- and two ß-subunits connected by disulfide bonds. The extracellular α-subunits contain the binding sites for IGF-1, whereas the transmembrane ß-subunits contain tyrosine kinase domains an adenosine triphosphate (ATP)-binding site. The IGF1R has a high affinity for both IGF-1 and IGF-2 and initiates, after activation through ligand binding, signaling cascades that result in regulation of a number of biological responses [38][40-44].

This biological activity of the IGF-1 protein is strongly influenced by binding proteins (IGFBP). These IGFBPs extend the half-life of IGFs and modulate their bioavailability as well as the delivery of the IGF to target organs. IGFBPs also regulate the activity of IGF through interactions with extracellular proteases which degrade IGFBPs. This results in the release of IGF and the activation of IGF1R. IGF-1 is bound with high affinity to a family of six specific IGFBPs (IGFBP-1 to 6). The serum concentrations of IGF are primarily affected by IGFBP3, which has the highest affinity for IGF-1 and IGF-2 and carries 80% of the circulating IGF-1. IGF which is bound by IGFBPs does not interact with receptors. Therefore, IGFBPs also inhibit and control the IGF signaling [38-42][45-46].

Circulating IGF-1 and IGF-2 bind to the IGF1R and trigger the activation of different signaling cascades, including the phosphatidylinositol 3-kinase (PI3K)–AKT–TOR pathway and the RAF–MAPK pathway, that stimulate cell proliferation and survival. The ligand binding to the IGF1R leads to autophosphorylation of the tyrosines 1131, 1135 and 1136 in the kinase domain of the receptor. This induces the phosphorylation of specific tyrosines and serines that form binding sites for docking proteins. Recruitment of these molecules activates the signaling pathway via the phosphatidylinositol-3-kinase (PI3K)-AKT and RAS/RAF/mitogen-activated protein kinase (MAPK) pathways. The intracellular IGF1R kinase activity is regulated by Src, integrins and protein phosphatases. Furthermore, several effectors (mTOR, mTORC1, p70, S6, ERK, JNK), acting downstream, are involved in the feedback suppression of the signaling pathway [20][38-41][43-44].

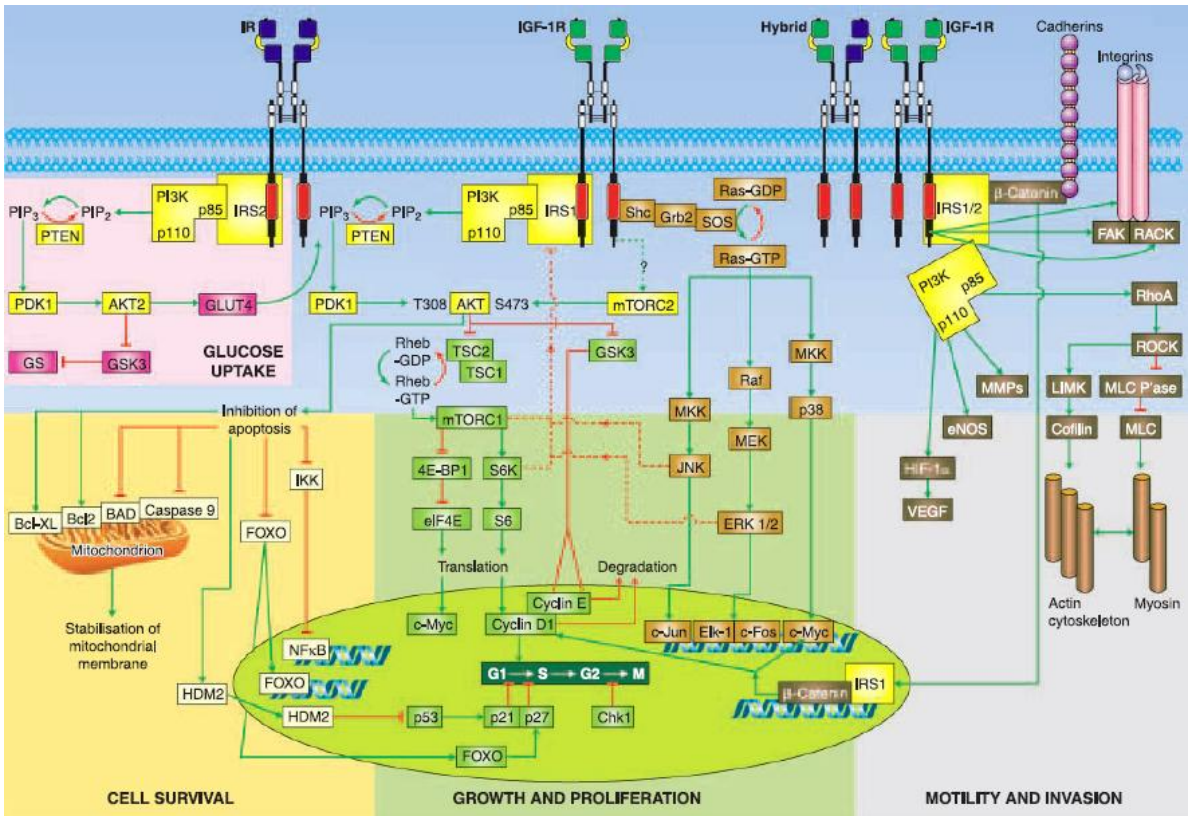

Fig.3: IGF-1 mediated signaling results in regulation of cell growth and proliferation, cell survival and motility, and invasion. Green lines show activation whereas red lines depict inhibition. The signaling downstream of IGF1R, insulin receptor (IR) and hybrid receptors, and their principal effectors is pictured. After IGF1R activation, regulatory (p85) and catalytic (p110) subunits of PI3K are recruited. PIP3 production activates PDK-1, which activates AKT. AKT is also activated by the mTORC2 complex, initiated by an unknown mechanism by the IGF1R. AKT promotes cell survival, stabilizes the mitochondrial membrane, inhibits apoptosis, induces the expression of pro-survival genes and blocks the expression and function of growth inhibitors. The mTORC1 complex enhances the translation of proteins involved in proliferation. Activation of RAS, RAF and mitogen-activated protein kinase isoforms ERKs, p38 and JNK, results in transcription of proliferative genes. Motility and migration are enhanced by cross-talk between the IGF1R and integrins, leading to actin reorganization and actin/myosin contractility. IGFs induce the expression of MMPs, for invasion and stimulate angiogenesis by activating endothelial nitric oxide synthase and induce expression of hypoxia-inducible factor-1a and vascular endothelial growth factor [41].

These pathways affect cell proliferation, apoptosis, differentiation, tissue homeostasis (Ras-Raf-Erk), cell survival, metabolic actions and differentiation (PI3K/Akt) (Fig.3). Akt can interact with nuclear transcription factors and plays a critical role in apoptosis by inhibiting pro-apoptotic proteins (BAD, FKHR) and by activating anti-apoptotic factors such as NF-kappaB and MDM2 [39-40][46]. Additionally it is known that IGF has protective functions in the heart [38-40]. The effects of an IGF-1 bound synthetic cell carrier (for use in transplantation studies) on mesenchymal stem / stroma cells have not been studied so far.

1.6 Aim of the Study

A caged NO-donor as well as the active site of the IGF-1-protein in a hydrogel was used for the generation of an extracellular environment to improve the survival and function of adipose derived mesenchymal stem / stroma cells (MSC) and to study the effect on myocardial infarction. The effects of both the nitric oxide and the active site of IGF-1 hydrogel on the proliferation of MSC and their angiogenic and anti-inflammatoric potential were studied *in vitro*. Furthermore, the effect of the hydrogel with additives on cell survival and heart regeneration was investigated in a mouse model.

2. Materials and Methods

2.1 Isolation of adipose derived MSC

2.1.1 Materials

Transgenic male FVB mice, 10 weeks old
Transgenic male C57 mice, 10 weeks old
Collagenase 1 (Gibco Life Technologies, NY, USA)
MEM α Medium basic (Gibco Life Technologies, NY, USA)
MEM α Medium + 20% FBS + 1% P/S
P/S 100 000U/l (tbd Science, Tianjin, China)
FBS (BI Biological Industries, Beit Haemek, Israel)
Cell culture dishes 100mmx20mm (Corning Incorporated, NY, USA)
Cell culture dishes 60mmx15mm (Corning Incorporated, NY, USA)
50ml centrifuge tubes (Corning Incorporated, NY, USA)
Cell strainer 40µm pore size (BD Biosciences, San Jose, California, USA)

2.1.2 Method

MSCs were isolated from male transgenic FVB and C57 mice that express firefly luciferase (Fluc) and green fluorescent protein (GFP) under the control of a CMV- or VEGF-promotor, respectively. The ubiquitously expressed GFP and Fluc can be detected in isolated MSC by fluorescent microscopy.

For isolation of MSCs visceral and gonadal adipose tissue were excised, digested and stored in basic MEM α medium. Afterwards tissues were washed twice in PBS to remove debris and blood. Tissues were cut into small pieces and PBS was added and tissues transfered into a 50ml centrifuge tube. After 10min of centrifugation at 1000rpm tissues floated on the PBS. The PBS was discarded and tissues were digested enzymatically for 60min in 10ml collagenase 1 (dissolved in basic MEM α medium at a concentration of 0.075%) on a shaking incubator at 37°C. Subsequently, 30ml basic MEM α medium was added for washing and centrifuged for 5min at 400rpm. The

supernatant (floating tissues and the medium) was removed and the pellet was washed twice in basic MEM α medium. Afterwards the pellet was resuspended in 5ml MEM α medium supplemented with 20% FBS and 1% P/S. Subsequently, the cell suspension was filtered through a 40µm cell strainer to remove the remaining tissue. The cell suspension was collected and seeded in cell culture dishes (60mmx15mm) and incubated for 3 days under standard conditions.

2.2 Culture of MSC

2.2.1 Materials

MEM α Medium (Gibco Life Technologies, NY, USA)

FBS (BI Biological Industries, Beit Haemek, Israel)

P/S 100 000 U/l (tbd Science, Tianjin, China)

Trypsin (Gibco Life Technologies, NY, USA)

DMSO (Sigma Aldrich, Munich, Germany)

Cell culture dishes 100mm x 20mm (Corning Incorporated, NY, USA)

Centrifuge tubes 50ml (Corning Incorporated, NY, USA)

Freezing vials (Corning Incorporated, NY, USA)

2.2.2 Method

MSC were cultured in MEM α medium supplemented with 20% FBS and 1% P/S in 10cm cell culture dishes. Medium was changed every second day. When cells reached confluency, they were washed with PBS and digested using 2ml trypsin for 3min at 37°C in the incubator. Afterwards, cells were harvested in 3ml medium and transferred in a 50ml centrifuge tube before they were centrifuged 5min at 1000rpm to pellet cells and to remove remaining trypsin in the supernatant. The pellet was resuspended in medium, split 1:5 and seeded on cell culture dishes (100mm x 20mm). In case that the cells were used for experiments, the pellet was resuspended in 3ml media and cells were counted in the Neubauer chamber. In case of storing cells in liquid nitrogen, the pellet was resuspended in ice-cold FBS containing 10% DMSO. Subsequently, cells were

stored at -80°C for at least 24h before the vials were transferred to liquid nitrogen. For thawing cells, warm medium was added to the vial containing the frozen cells. Then, the cell suspension was transferred to a 50ml tube and centrifuged at 1000rpm and the supernatant discarded to remove the DMSO. Afterwards the cell pellet was resuspended in MEM α medium and seeded on cell culture dishes.

2.3 Synthesis of the Active Site of IGF-1 Linked to NapFFG

2.3.1 Materials

Resin	1.5mmol/g (GL Biochem, Shanghai, China)
Threonin (T)	Fmoc-Thr(tBu)-OH, 397.48mmol (GL Biochem, Shanghai, China)
Glutamine (Q)	Fmoc – Gln(Trt)-OH, 610.7mmol (GL Biochem, Shanghai, China)
Proline (P)	Fmoc-Pro-OH, 337.38mmol (GL Biochem, Shanghai, China)
Alanine (A)	Fmoc-Ala-OH, 312.3mmol (GL Biochem, Shanghai, China)
Arginine (R)	Fmoc-Arg(Pbf)-OH, 648.77mmol (GL Biochem, Shanghai, China)
Serine (S)	Fmoc-Ser(tBu)-OH, 384mmol (GL Biochem, Shanghai, China)
Glycine (G)	Fmoc-Gly-OH, 292.3mmol (GL Biochem, Shanghai, China)
Tyrosine (Y)	Fmoc-Tyr-OH, 403.43mmol (GL Biochem, Shanghai, China)
Phenylalanine (F)	Fmoc-Phe-OH, 387.4mmol (GL Biochem, Shanghai, China)
2-Naphthalenacetic Acid (Nap) 99%, 186.2g/mol (Aladdin, Shanghai, China)	
HBTU	379mmol (GL Biochem, Shanghai, China)
N-N-Diisopropylethylamine (DIEA) (J&K scientific LTD, Beijing, China)	
Dichlormethane (HuaDong Product, Tianjin, China)	
Methanol (Chemical Reagent, Tianjinshi Yuanli Chemical Co. LTD, Tianjin, China)	
Dimethylformamide (DMF) (Chemical Reagent, Tianjinshi Yuanli Chemical Co. LTD, Tianjin, China)	
Hexahydropyridine (Sinupharm Chemical Reagent Co. LTD, Shanghai, China)	
20% Piperidine (Hexahydropyridine in DMF)	
Trifluoro acetic acid (TFA)(J&K scientific LTD, Beijing, China)	
Triisopropylsilane (Tris)97% (J&K scientific LTD, Beijing, China)	
Ether absolute 99% (Chemical Reagent, Tianjinshi Yuanli Chemical Co. LTD, Tianjin,	

China)

Syringe filter, 13mm 0.45µm pore size (Ameritec Scientific Corporation, Tianjin, China)

Venusil XBP C18 column (Agela Technologies, Tianjin, China)

2.3.2 Method

The active site of the IGF-1 protein consists of a 12 amino acids with the sequence GYGSSSRRAPQT [47]. This was linked to the hydrogel forming sequence NapFFG to construct an IGF-1-hydrogel as extracellular environment (Fig.4).

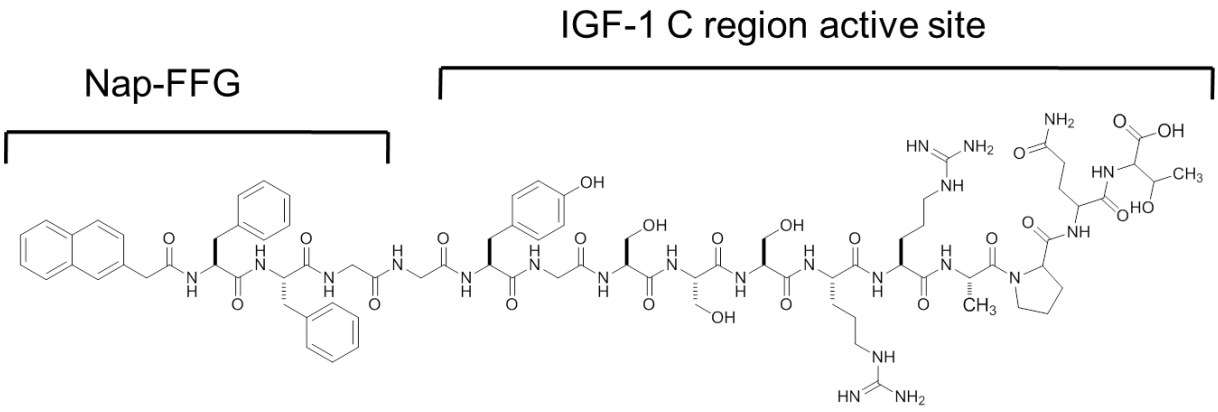

Fig.4: Structure of the active site of the IGF-1 protein linked to the gel forming compound NapFFG.

For the synthesis of the IGF-1 active site and the gel-forming compound NapFFG, 0.5g resin was dissolved in CH_2Cl_2 and mixed in the solid phase synthesis glass reaction vial for 5min on a transference decoloring shaker TS-8 (Ningbo Hinotek Technology Co. Ltd, Zhejiang, China). One g resin is able to bind 1.5mmol amino acids. Consequently, 1mmol (at least 0.75mmol) of the first amino acid threonin was dissolved in CH_2Cl_2 with 330µl of DIEA and added to the resin and incubated for 1h. Afterwards, the remaining binding sides were blocked by washing with CH_2Cl_2-MeOH-DIEA-solution (17:2:1) for 10min. Subsequently, the solution was washed twice with CH_2Cl_2 for 60sec and five times with DMF each for 60sec. Before another amino acid could be added, the Fmoc-protecting-group had to be removed by washing with 20% Piperdine solution

for 30min and five times washing with DMF for 60sec. Afterwards, the next amino acid in the sequence (Q) was mixed with HBTU and DIEA (AA:HBTU:DIEA=2:2:4), dissolved in DMF and was allowed to bind for 2h. After five additional washing steps with DMF the Fmoc-protecting-group on the added amino acid was removed. After the fifth amino acid, the amino acids were added twice to guarantee the binding: after2h incubation the solution was washed with DMF for three times and the amino acid mixed with HBTU and DIEA (AA:HBTU:DIEA=1:1:2) dissolved in DMF was added again and incubated for another hour. This was performed until the last amino acid in the sequence was added and the peptide was washed for five times in DMF and another five times with CH_2Cl_2. Subsequently, the synthesized peptide was incubated for 30min in a TFA-Tris-H_2O-solution (95:2.5:2.5) to remove the resin. The solution including the peptide was collected in a round bottom flask and the remaining resin was washed again three times in DMF to collect the synthesized peptide. The solution was concentrated in the Rotavapor (R-210, BÜCHI, Switzerland) for about 30min. Afterwards, 25ml ether absolute were added and the round bottom flask was put on ice until the peptide precipitated. The remaining solution was discarded and the powder was dried using an air pump (ACO-002, SenSen, Zhejiang, China) under a flow of 40l/min. A sample of the powder was dissolved in methanol and cleaned through a 0.45µm syringe-filter before it was injected in the UFLC (UFLC DGU-20A3, Shimadzu, Beijing, China) for determination of its peptide mass (1784.8271). The binary solvent system of the UFLC separation is shown in table 2. Solution A was composed of H_2O + 0.035% TFA whereas solution B was composed of CH_3CN + 0.035% TFA.

Tab.1: Eluation-program for LC-MS mass detection

Time	0-2.5min	2.5-5min	5-8min	8-9min	9-10min
Solution A	90%	55%	0%	0%	90%
Solution B	10%	45%	100%	100%	10%

The peptide was purified by HPLC (LC3000, CXTH, Beijing,China) using a C18 column at a flow of 8ml/min. Therefore, 0.8mg powder was dissolved in 4ml DMSO. The solvent

system used for the separation of the substances is shown in table 3. Solution A was composed of 95% H_2O + 5% CH_3OH + 0.05% TFA whereas solution B consisted of CH_3OH + 0.05% TFA. For each separation 400µl of the peptide solution were applied onto the system. The NapFFG-IGF-1-peptide was collected after 18min. Eluates were freeze-dried (Christ alpha 1-4 LD, John Morris Scientific, Chatswood, NSW, Australia). The remaining powder was stored at -18°C until use.

Tab.2: Eluation-program for the purification using HPLC

Time	0-17min	17-18min	18-25min	25-30min	30min
Solution A	70%	10%	0%	70%	70%
Solution B	30%	90%	100%	30%	30%

2.4 Preparation of the Hydrogel

2.4.1 Materials

NapFFG-powder containing a caged NO-donor (Key Laboratory of Bioactive Materials, Nankai University)

NapFFG-powder (Key Laboratory of Bioactive Materials, Nankai University)

NapFFG-IGF-1 powder

0.9% Sodium chloride (Cisen Pharmaceutical Ltd, Jining, Shandong, China)

Na_2CO_3 105.99g/mol (Benchmark, Houston, Texas, USA)

Syringefilter acrodisc 0.2µm (Pall life science, Ann arbor, MI, USA)

2.4.2 Method

The NapFFG-powder as well as the NapFFG-powder containing a caged NO-donor was provided by Dr. Gao Jie of the Key Laboratory of Bioactive Materials at Nankai University, China [48].

A 1% hydrogel solution (in 0.9% saline) was adjusted to pH 7.2-7.4 with sterile 1M Na_2CO_3 solution (in 0.9% saline). To obtain a clear homogenous solution, the hydrogel solution was heated to 70°C and cooled down to room temperature to form a gel. The hydrogel solution was stored at 4°C until experimental use.

2.5 *In Vitro* Studies

2.5.1 MTT Cell Proliferation Assay

2.5.1.1 Materials

NapFFG containing a caged NO-donor (Key Laboratory of Bioactive Materials, Nankai University)
NapFFG (Key Laboratory of Bioactive Materials, Nankai University)
NapFFG-IGF-1
ß- Galactosidase; 3.9 units/mg (Sigma Aldrich, Munich, Germany)
MEM α-Medium (Gibco Life Technologies, NY, USA)
MTT powder M2128 (Sigma Aldrich, Munich, Germany)
DMSO (Chemical Reagent, Tianjinshi Yuanli Chemical Co. LTD, Tianjin, China)
96-well plate Costar 3599 (Corning Incorporated, NY, USA)
Syringefilter acrodisc 0.2µm (Pall life science,Ann Arbor, MI, USA)

2.5.1.2 Method

For the MTT-Cell Proliferation Assay 3000 cells/well in 100µl media or hydrogel (NapFFG, NapFFG-IGF-1, NapFFG with caged NO-donor, diluted 1:100 in media) were seeded in a 96 well plate. Then, 100U/l ß-Galactosidase was added to the media including the hydrogel with the caged NO-donor. The medium was changed every second day. After 24h, 48h and 72h the medium was removed and 100µl MEM α-medium and 20µl MTT were added to each well. After 4h of incubation cells were washed with PBS and 150µl DMSO was added. Then plates were incubated for 15min on an orbital shaker (Liuyi WD 9405B, Beijing, China). Subsequently, 50µl of the liquid

was transferred to 96-well plate and the absorbance was measured at 490nm using a microplate reader (BioRad, iMark, Berkley, California, USA).

2.5.2 Reverse Transcription-qPCR

2.5.2.1 Materials

NapFFG containing a caged NO-donor (Key Laboratory of Bioactive Materials, Nankai University)
NapFFG (Key Laboratory of Bioactive Materials, Nankai University)
NapFFG-IGF-1
ß- Galactosidase; 3,9 units/mg (Sigma Aldrich, Munich, Germany)
MEM α-Medium (Gibco Life Technologies, NY, USA)
H_2O_2 (Chemical Reagent, Tianjinshi Yuanli Chemical Co. LTD, Tianjin, China)
DEPC H_2O (Beyotime, Shanghai, China)
Ethanol (Chemical Reagent, Tianjinshi Yuanli Chemical Co. LTD, Tianjin, China)
Chloroform (Chemical Reagent, Tianjinshi Yuanli Chemical Co. LTD, Tianjin, China)
Isopropylalcohol (Chemical Reagent, Tianjinshi Yuanli Chemical Co. LTD, Tianjin, China)
TransZol (Transgen, Beijing, China)
TriZol (Transgen, Beijing, China)
Oligo d(T) 18, 14nm (Takara Bio Inc.,Shiga, Japan)
dNTPs, 2,5mM each (Transgen, Beijing, China)
Recombinant RNasin RNase Inhibitor; 40U/µl (Promega, Madison, WI, USA)
M-MI V Reverse Transcriptase 200U/µl (Promega, Madison, WI, USA)
M-MLV RT 5x Buffer (Promega, Madison, WI, USA)
mVEGFa-Primer (AOKE, Beijing, China)
mSDF-1-Primer (AOKE, Beijing, China)
GAPDH-Primer (AOKE, Beijing, China)
Fast Start Universal SYBR Green Master Rox (Roche Diagnostics, Mannheim, Germany)

2.5.2.2 Method

For the RT-qPCR, 150,000 MSC/well were seeded in a 6 well plate and cultured for 24h in MEM α medium. Then, cells were incubated with 100µl MEM α without FBS but containing 100µM H_2O_2 to mimic ischemic conditions. As a control cells were incubated with MEMα alone. After 1h the medium was changed to medium containing NapFFG, NapFFG-IGF-1 or NapFFG with caged NO-donor (diluted 1:100) and as a control medium alone for another 24h. Furthermore, to the media containing the hydrogel with the caged NO-donor, 100U/l ß-galactosidase was added to trigger NO-release. Then, cells were washed with PBS. For RNA isolation 1ml TransZol was added to each well and incubated for 5min. Then, the solutions were transferred to Eppendorf-vials and 200µl chloroform was added. After 2min of incubation solutions were centrifuged for 7min at 12,000rpm in an Eppendorf Centrifuge 5417R. The supernatants were collected and an equal volume isopropylalcohol was added and incubated for 10min. Subsequently, the solutions were centrifuged and pellets washed twice with 70% EtOH before they were dried for 15min. Afterwards, 15µl TriZol RNA dissolving solution was added to each pellet and incubated at 70°C for 5min. The concentrations of the RNA were determined at 240nm using Thermo Scientific Nano Drop 2000 (Wilmington, USA).

For cDNA synthesis, 2µg RNA were mixed with 1µl Oligo d(T) and DEPC H_2O to get a total volume of 10.7µl. Then, samples were incubated at 72°C for 6min and cooled down on ice for 2min before 9.3µl of the mastermix was added to get a total volume of 20µl. The mastermix contained 4µl dNTPs, 0.5µl RNase inhibitor, 0.8µl reverse transcriptase and 4µl 5x buffer per sample. The RNA was reverse transcribed in an Eppendorf Mastercycler (Hamburg, Germany) for 1h at 42°C, 5min at 95° and stored at 4°C.

Primers (Tab.4) were dissolved in ddH_2O at a concentration of 10µM. For qRT-PCR 1µl of the forward as well as the reverse primer were added to 10µl SYBR-Green mix, 1µl cDNA and 7µl ddH_2O to give a final volume of 20µl. 40 cycles (Fig.5.) were applied in the thermo cycler BioRad CFX Connect RealTime System (Berkley, California, USA). Glyceraldehyde-3-phosphate dehydrogenase (GAPDH) is ubiquitously expressed and was used as housekeeping gene.

Tab.3: Primers used for RT-PCR

Gene	Forward primer	Reverse primer
mVEGFa	5'-GTCGGAGAGCAACGTCACTA-3'	5'-TCTCCTATGTGCTGGCTTTG-3'
mSDF-1	5'-TATAGACGGTGGCTTTGA-3'	5'-TTGACTCAGGACAAGGCATC-3'
mGAPDH	5'-GTCAAGCTCATTTCCTGGT-3'	5'-CCAGGGTTTCTTACTCCTTG-3'

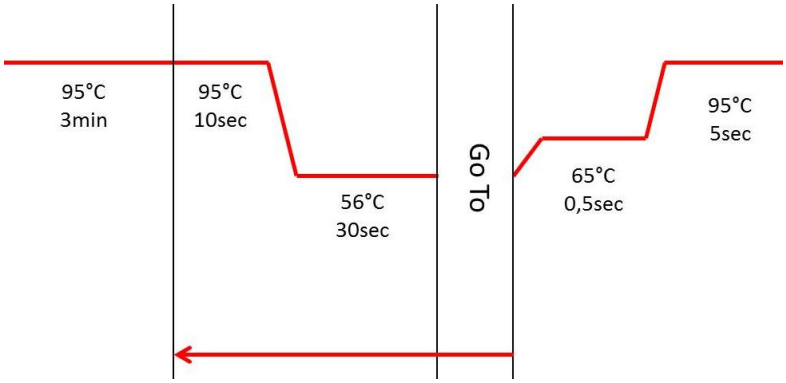

Fig.5: Temperature schema for qPCR

2.6 *In vivo* Studies

2.6.1 C57 Cell Labeling

2.6.1.1 Materials

MEM α Media (Gibco Life Technologies, NY, USA)

Trypsin (Gibco Life Technologies, NY, USA)

PKH26 Red Fluorescent Cell Linker Kit (Sigma Aldrich, Munich, Germany)

0.9% Sodium chloride (Cisen Pharmaceutical Ltd, Jining, Shandong, China)

2.6.1.2 Method

MSC isolated from C57 mice express GFP and Fluc under the control of a VEGF-R-promoter. Consequently, in the absence of VEGF no GFP signal can be detected. Therefore, the cells were labeled with the PKH26 cell membrane labeling dye to be detectable in mice.

Cells were washed with PBS before they were digested with trypsin as previously described. A PKH26 Red Fluorescent Cell Linker Kit was used according to the manufacturer's instructions. Cell suspension was washed with medium not containing FBS and centrifuged for 5min at 1000rpm. The pellet was resuspended in 1ml Diluent C, contained in the kit, and mixed with 4µl PKH26 dye solution in 1ml Diluent C to give a final volume of 2ml. Cells were stained for 5min while mixing periodically. Subsequently, 10ml medium containing FBS was added to stop the staining reaction and cells were pelleted by centrifugation at 1,000rpm for 10min. The cells were washed 3 times in medium before they were resuspended in sodium chloride and used for animal surgery.

2.6.2 Animal Surgery

2.6.2.1 Materials

FVB mice, female, 8 weeks old

C57 mice, female, 8 weeks old

MEM α Medium (Gibco Life Technologies, NY, USA)

Trypsin (Gibco Life Technologies, NY, USA)

0.9% Sodium chloride (Cisen Pharmaceutical Ltd, Jining, Shandong, China)

ß- Galactosidase; 3,9 units/mg (Sigma Aldrich, Munich, Germany)

Isoflurane (Abbott Laboratories, Illinois, USA)

3-8 silk twine (NingBo cheng-he microsurgical instruments, China)

7-0 silk twine (NingBo cheng-he microsurgical instruments, China)

Gentamycin sulfat injection (Bicon pharmaceutical, Jiangsu, China)

2.6.2.2 Method

All animal experiments were approved by the Animal Care and Ethics Committee of the Nankai University, China. Animals were purchased from the Laboratory Animal Center of the Academy of Military Medical Sciences (Beijing, China) and were cared for according to the regulations of the Administration of Affairs Concerning Experimental Animals (Tianjin, revised in June 2004). Animal experiments and surgery were performed in cooperation with Dr. Yi Liu, Nankai University, China.

Eight-weeks old female FVB as well as C57 mice were used for artery ligation and randomized into 3 groups receiving MSC-treatment, MSC in NapFFG-hydrogel and MSC in NO-releasing hydrogel. Injection of MSC in IGF-1-NapFFG-hydrogel was not possible, due to the loss of the gel consistency after mixing the hydrogel with the cells.

MSC at passage 3 were collected with trypsin as previously described, counted and resuspended in sodium chloride. For the treatment with MSC in hydrogel, a 1% hydrogel was used and mixed 1:1 with the cell suspension to obtain a 0.5% hydrogel containing MSC. ß-Galactosidase was dissolved in 0.9% sodium chloride to obtain a 100U/l ß-Galactosidase solution.

FVB mice were anaesthetized by inhalation of 5% isoflurane with a frequency of 120 breaths per minute (BPM). Then, mice were intubated and mechanical ventilated with 2% isoflurane using an anaesthetic machine (Hallowell EMC MicroVent 1, Pittsfield, MA, USA). The chest was opened with a scissor and kept open with a rib- and sternum-retractor. Afterwards, the left anterior descending coronary artery was permanently ligated using a 7–0 silk suture. Infarction was considered successful through the visual appearance of pale discoloration. Immediately after the ligation $2x10^5$ MSC in 20µl cell suspension were injected into the 2 areas adjacent to the infarcted tissue. Each mouse received two injections of $1x10^5$cells in 10µl each. Subsequently, mice were closed with a 3-8 silk twine (stored in sodium chloride). Then, 100µl of a 100U/l ß-Galactosidase solution was injected through the mouse's tail vein to trigger the NO release. Mice without NO-hydrogel treatment received the ß-galactosidase injection as a control. After termination of anesthesia, animals woke up after 3minutes while recovering on a breathing machine (ALC-V85). Operated mice

were not allowed to feed for the first night and got water with 0.1% gentamycin. Mice received another injection of ß-galactosidase on day 3 after surgery to boost NO-release.

2.6.3 Molecular Imaging and Cell Tracking in Living Animals

2.6.3.1 Materials

D-Luciferin (SynChem, Shanghai, China)

Isoflurane (Abbott Laboratories, Illinois, USA)

2.6.3.2 Method

The molecular imaging for cell tracking was performed every second day, starting on day 1 until day 7. One hundred µl of the substrate D-luciferin were injected into the peritoneum of FVB mice before they were anaesthetized through inhalation of 5% isoflurane with a frequency of 120 breaths per minute (BPM) using an anaesthetic machine (Caliper Life Sciences, Xenogen XGI-8, Hopkinton, Massachusetts, USA). After 10min mice were transferred in the molecular imaging machine (Caliper Life Sciences, IVIS Lumina II, Hopkinton, Massachusetts, USA) and the luminescence signal was detected during a 5min exposure time.

2.6.4 Collection of the Infarcted Heart

2.6.4.1 Materials

0.9% Sodium chloride (Cisen Pharmaceutical Ltd, Jining, Shandong, China)

Ethanol absolute (Chemical Reagent, Tianjinshi Yuanli Chemical Co. LTD, Tianjin, China)

Trichlormethane (Chemical Reagent, Tianjinshi Yuanli Chemical Co. LTD, Tianjin, China)

Acetic acid (Chemical Reagent, Tianjinshi Yuanli Chemical Co. LTD, Tianjin, China)

2.6.4.2 Method

At day 7 and day 30 mice were sacrificed. Hearts were rinsed with a saline injection in the right ventricle until the tissue turned pale. Adjacent tissue was removed and hearts were washed in saline before they were fixed for 6-7h in the fixing solution consisting of 60% ethanol, 30% trichlormethane and 10% acetic acid at 4°C. Subsequently, tissues were washed in ethanol absolute, incubated in 70% ethanol until the tissue was dehydrated in a tissue processor (Leica ASP200S, Nussloch, Germany) and paraffin embedded. The tissue of the heart, proximal from the knot was selected (tissue distal from the knot was discarded). Slices (5µm) were prepared and collected on slides in the order of sectioning.

2.6.5 Histological Analysis

2.6.5.1 Materials

Xylene 1 (Chemical Reagent, Tianjinshi Yuanli Chemical Co. LTD, Tianjin, China)
Xylene 2 (Chemical Reagent, Tianjinshi Yuanli Chemical Co. LTD, Tianjin, China)
Ethanol (Chemical Reagent, Tianjinshi Yuanli Chemical Co. LTD, Tianjin, China)

2.6.5.2 Method

For histological analysis the paraffin of each tissue slice was removed by incubation with Xylene 1 solution for 10min and another 10min in Xylene 2 solution. After a 15min drying step, tissue slices were rehydrated for 5min in 99% EtOH, 95% EtOH, 90% EtOH and 85% EtOH. Subsequently, tissue slices were washed in tap water for 5min before staining.

2.6.5.2.1 HE Staining

2.6.5.2.1.1 Materials

Hematoxylin (Lian Xing, Tianjin, China)
Eosin (Lian Xing, Tianjin, China)
Ethanol (Chemical Reagent, Tianjinshi Yuanli Chemical Co. LTD, Tianjin, China)
HCl (Chemical Reagent, Tianjinshi Yuanli Chemical Co. LTD, Tianjin, China)
Xylene 1 (Chemical Reagent, Tianjinshi Yuanli Chemical Co. LTD, Tianjin, China)
Xylene 2 (Chemical Reagent, Tianjinshi Yuanli Chemical Co. LTD, Tianjin, China)
Neutral Balsam (ZSGB-Bio OriGene, Beijing, China)

2.6.5.2.1.2 Method

For the HE staining slides 10 and 20 after the knot were used. Rehydrated tissue slices were stained for 15min in Hematoxylin, rinsed for 5min with running tap water and differentiated for 1sec in CH_3CH_2OH-HCl before the tissue slices were rinsed for 5min. Afterwards, tissue slices were stained in Eosin for 30sec and rinsed for 5min with running tap water. Subsequently, the tissues were shortly dehydrated in 85% EtOH, 90% EtOH, 95% EtOH and left for 3min in 99% EtOH, 5min in Xylene 1 and another 5min in Xylene 2. Then, tissue slices were dried and mounted using Neutral Balsam. Afterwards, pictures at 2.5x magnification were taken on an Olympus SZ61 microscope and *Sharp Capture* Imaging Software.

2.6.5.2.2 Masson's Trichrome Staining

2.6.5.2.2.1 Materials

Masson (Lian Xing, Tianjin, China)
Acetic acid (Chemical Reagent, Tianjinshi Yuanli Chemical Co. LTD, Tianjin, China)
Phosphotungsticacid (GuangFu Chemical Institute, Tianjin, China)
Bright Green (Lian Xing, Tianjin, China)

Ethanol (Chemical Reagent, Tianjinshi Yuanli Chemical Co. LTD, Tianjin, China)

Xylene 1 (Chemical Reagent, Tianjinshi Yuanli Chemical Co. LTD, Tianjin, China)

Xylene 2 (Chemical Reagent, Tianjinshi Yuanli Chemical Co. LTD, Tianjin, China)

Neutral Balsam (ZSGB-Bio OriGene, Beijing, China)

2.6.5.2.2.2 Method

For the Masson's Trichrome staining slides 9 and 19 after the knot were used. The rehydrated tissue slices were stained in the Masson solution containing 0.2% acetic acid for 4min and subsequently differentiated in phosphotungsticacid containing 0.2% acetic acid. Afterwards tissue slices were shortly washed before staining with Bright Green containing 0.2% acetic acid. Immediately after a short washing step in water the tissue slices were dehydrated in 85% EtOH, 90% EtOH, 95% EtOH and left for 3min in 99% EtOH, 5min in Xylene 1 and another 5min in Xylene 2 before they were dried and mounted using Neutral Balsam. Afterwards, pictures at 2.5x magnification were taken on an Olympus SZ61 microscope and *Sharp Capture* Imaging Software.

2.7 Statistical Analysis

Cell tracking pictures were analyzed using the *Living Image Analysis* Software (Caliper Life Sciences, Hopkinton, Massachusetts, USA). Microscope pictures were analyzed using GIMP 2.8. All data are expressed as mean ± standard deviation. Statistical significant differences were analyzed using paired Student's *t*-test. *** indicates $p < 0.001$, ** indicates $p < 0.01$ and * indicates $p < 0.05$.

3. Results

3.1 Analysis of NapFFG-IGF-1 Peptide by LC-MS

The purity of the synthesized NapFFG-IGF-1 peptide was analyzed by LC-MS (Fig.6).

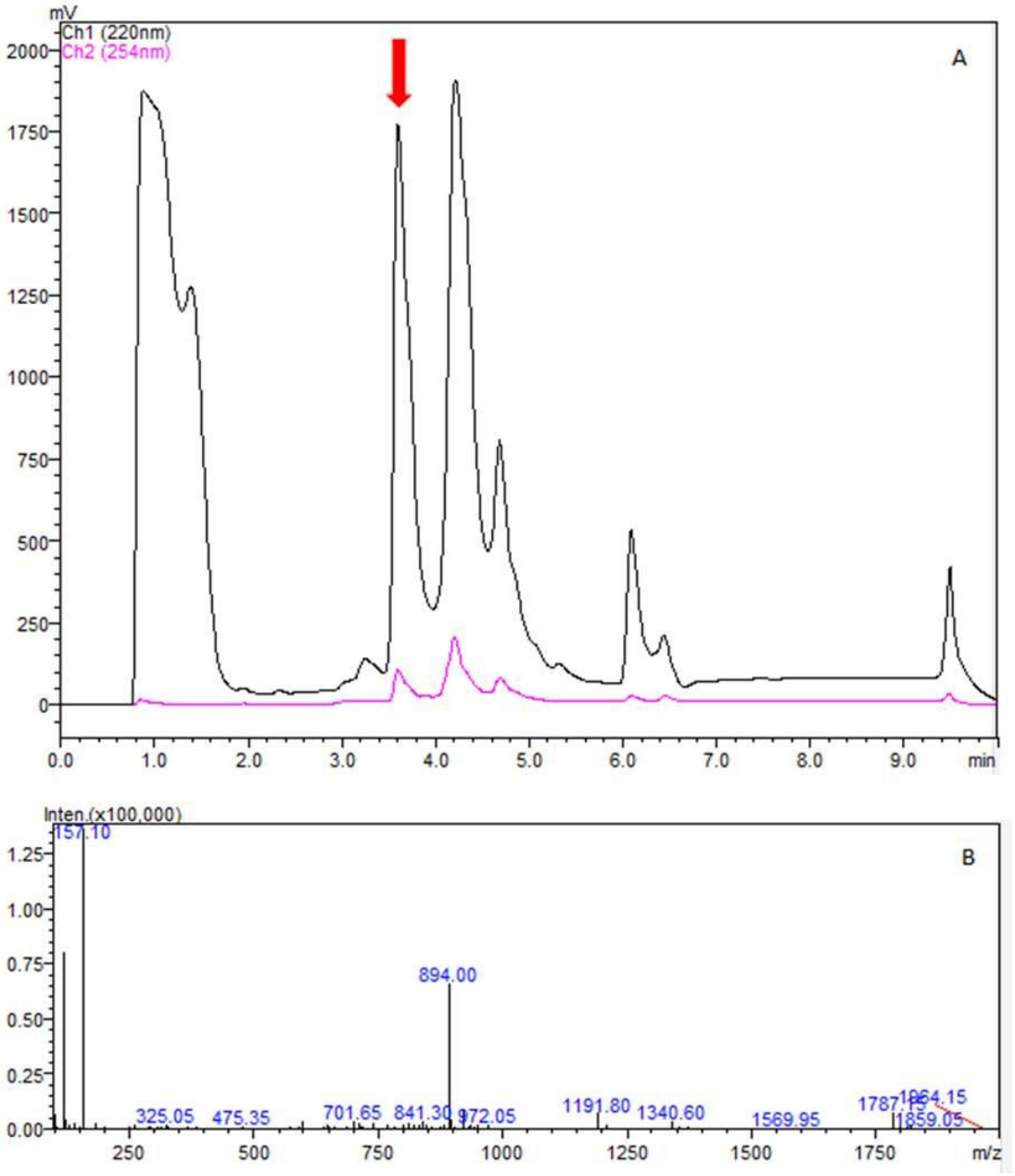

Fig.6: LC-MS analysis of the NapFFG-IGF-1 active site hydrogel powder. The NapFFG-IGF-1 active site hydrogel was separated on a reverse phase HPLC and the eluent monitored at 220nm and 254nm (A). The mass spectrumof the eluent at ~3.5 min is depicted in (B).

In the LC-MS chromatogram the NapFFG-IGF-1 active site peptide eluted at a retention time of ~3.5min (see Fig. 6A, indicated by an arrow). The m/z of the eluent at 3.5min was 894.00 (see Fig. 6B).

3.2 Proliferative Effects of Nitric Oxide and the Active Site of IGF-1 - Hydrogel on MSC

The effect of NapFFG-NO, NapFFG-IGF-1 and as a control NapFFG, on MSC viability was analyzed using the MTT proliferation assay. The MTT reagent was added after 24h, 48h and 72h and the absorbance of the reduced MTT tetrazole determined.

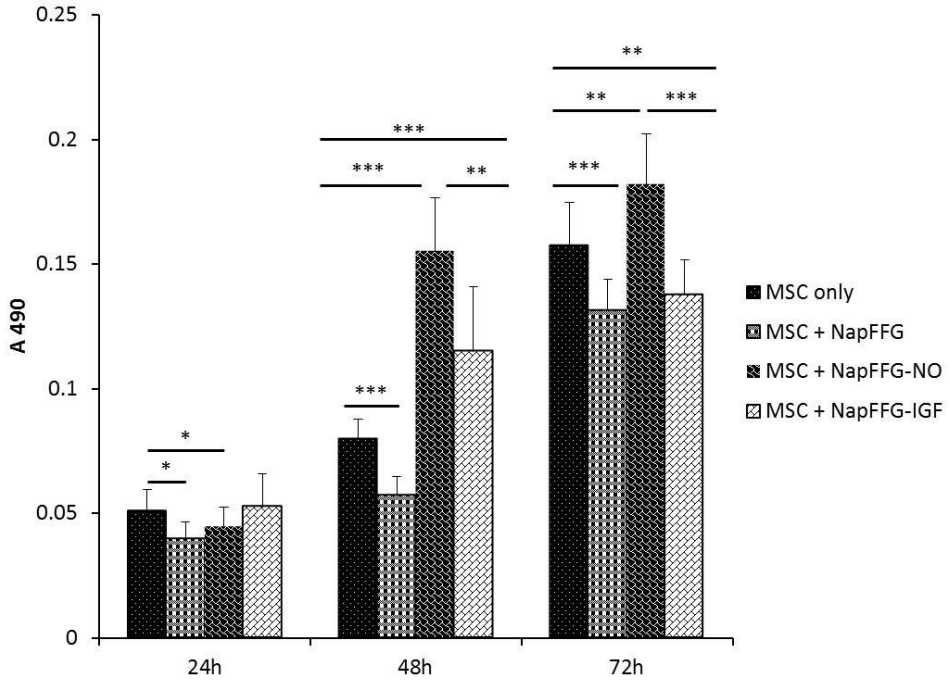

Fig.7: Effect of NapFFG-NO and NapFFG-IGF on the proliferation of MSC. MSC were incubated with MEM-α-medium, medium containing NapFFG, NapFFG-NO or NapFFG-IGF-1. After 24h, 48h and 72h the MTT reagent was added, and the absorbance of the reduced MTT tetrazole determined at 490nm. Data are mean + SD (n=4, *** p <0.001, ** p <0.01, * p <0.05).

Cells incubated for 24h (MSC only = control) showed an absorbance of 0.051 (±0009). MSC incubated with NapFFG and NapFFG-NO revealed a slightly reduced number of viable cells (with an absorbance of 0.039 ±0.007 in case of MSC + NapFFG and 0.045 ±0.008 in case of MSC + NapFFG-NO) while there was no significant difference between the control group and the MSC + NapFFG-IGF-1.

After 48h of incubation the MSC control group (MSC only) showed an absorbance of 0.078 ±0.008. NapFFG treatment significantly decreased the number of viable cells, resulting in an absorbance of 0.057 ±0.008 while NapFFG-NO and NapFFG-IGF-1 increased the cell proliferation significantly to an absorbance of 0.155 ±0.021 and 0.115 ±0.026, respectively. Furthermore, the absorbance of the reduced MTT tetrazole of MSC incubated with NapFFG-NO (0.155 ±0.021) was significantly higher than the absorbance of MSC incubated with the NapFFG-IGF-1 (0.115 ±0.026).

After 72h of incubation the reduced MTT tetrazole of the MSC control group (MSC only) gave an absorbance of 0.157 ±0.017. Again NapFFG and NapFFG-IGF-1 treatments led to decreased numbers of viable cells as evident by the absorbance of 0.131 ±0.013 and 0.138 ±0.014. However, MSC treated with NapFFG-NO showed a significant higher proliferation as compared to the control (MSC only), as evident by increased absorbance of 0.182 ±0.02.

3.3 Angiogenic Potential of the Nitric Oxide Releasing Hydrogel and of the IGF-1-active Site Hydrogel

MSC were examined for their expression of VEGF when incubated in MEM-α-medium (control), medium containing NapFFG, medium containing NapFFG-NO and medium containing NapFFG-IGF-1, under normal as well as under ischemic conditions (in the presence of H_2O_2), to estimate their angiogenic potential.

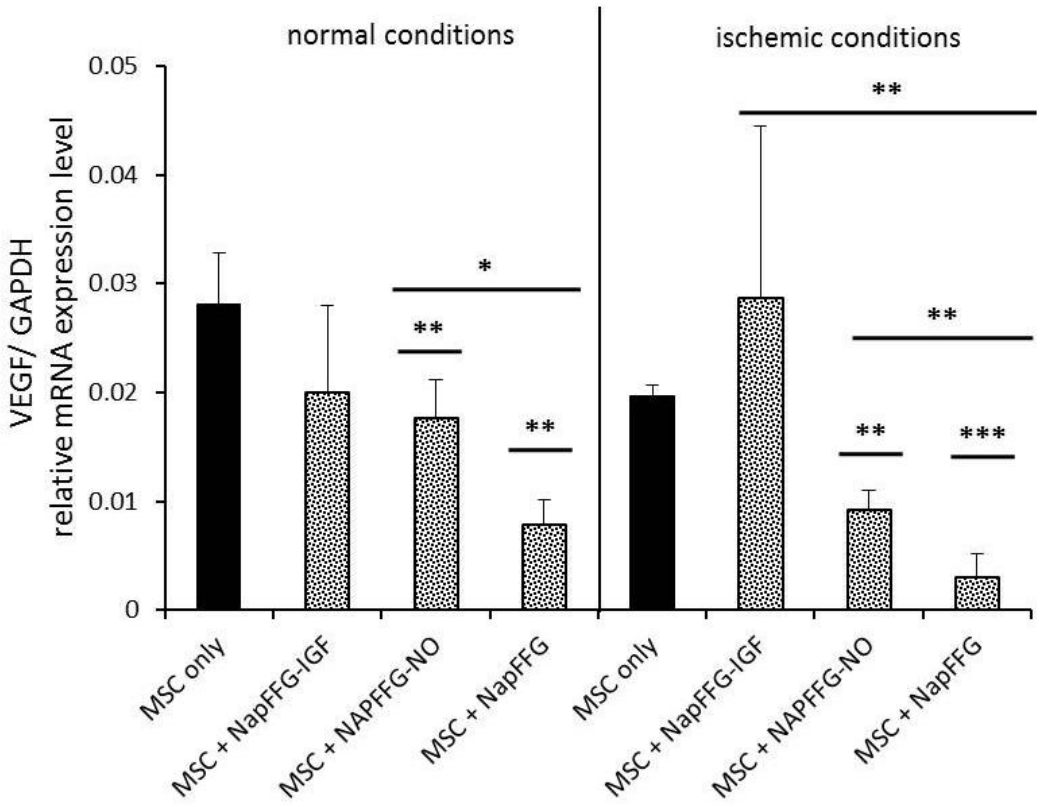

Fig.8: Relative mRNA expression level of VEGF in MSC. VEGF mRNA expression levels were determined by qRT-PCR in MSC cultured for 24h in MEM-α-medium (MSC only = control), medium containing NapFFG-NO, NapFFG-IGF-1 or NapFFG. Incubations were performed under standard ("normal") conditions and under ischemic conditions as mimicked by the presence of H_2O_2. Relative expression levels of VEGF were calculated using the quantification cycle (Cq), that represents the number of cycles necessary to reach a threshold signal level and were normalized to GAPDH expression level. Data are mean + SD (n=3, *** p <0.001, ** p <0.01, * p <0.05).

Under normal (standard tissue culture) conditions no significant difference in the relative VEGF expression between the MSC control group (MSC only, 0.028 ±0.005) and MSC treated with NapFFG-IGF-1 (0.0199 ±0.008) was determined (Fig. 8). However, the relative VEGF expression in MSC treated with NapFFG-NO (0.0176 ±0.004) and in MSC with NapFFG (0.0078 ±0.0024) was significantly lower than that in the MSC control group.

Under ischemic conditions no significant difference in the relative VEGF expression between the MSC control group (0.0197 ±0.0009) and MSC treated with NapFFG-IGF-1 with a relative VEGF expression of 0.0286 ±0.0158 was determined. In the NapFFG-NO treated group the relative VEGF expression (0.0091 ± 0.0019) was significantly lower than in the MSC control group. In addition, in the NapFFG treated group the VEGF expression (0.0029 ±0.00219) was significantly lower than in the MSC control group.

However, under "normal" conditions the relative VEGF expression of MSC cultured with NapFFG-NO was significantly higher than in MSC cultured with NapFFG alone. Furthermore, under ischemic conditions MSC treated with NapFFG-IGF-1 and NapFFG-NO revealed both a significant higher relative expression of VEGF than MSC treated with NapFFG.

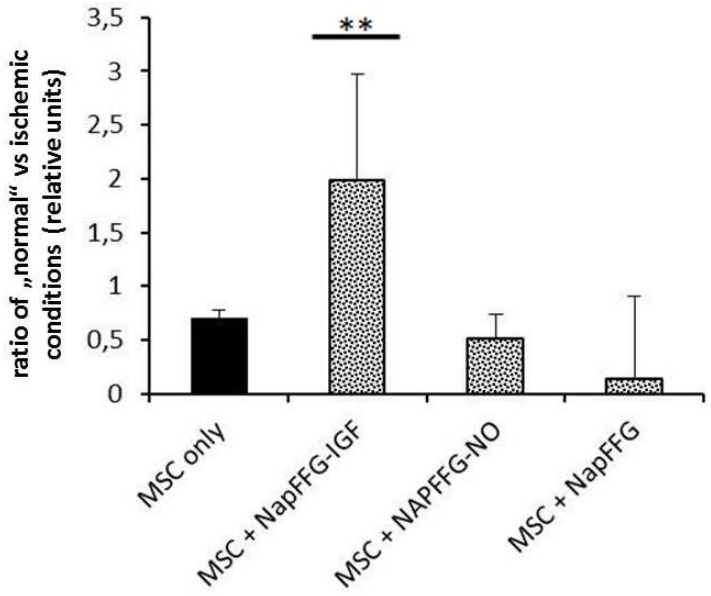

Fig.9: VEGF mRNA expression level in MSC upon treatment. VEGF mRNA expression levels were determined by qRT-PCR in MSC cultured for 24h in MEM-α-medium (MSC only = control), medium containing NapFFG-IGF-1, NapFFG-NO, or NapFFG, under "normal" (standard cell culture) as well as under ischemic conditions as mimicked by the presence of H_2O_2. The ddCt was calculated using GAPDH expression as a control and the ratio between of untreated and treated cells termed as "normal" and ischemic conditions was calculated. Data are mean + SD (n=3, ** p <0.01).

In comparison to the MSC control group (0.705 ±0.073), the ratio ddCt of the NapFFG-IGF-1 treated MSC was significantly higher (1.985 ±0.984). There was no significant effect of NapFFG-NO (0.509 ±0.223) or NapFFG treatment of MSC (0.145 ±0.765) (Fig. 9).

3.4 Anti-inflammatory Potential of a Nitric Oxide Releasing Hydrogel and the IGF-1-active Site Hydrogel

MSC were analyzed for their expression of SDF-1. To determine the anti-inflammatory potential of NapFFG-NO and NapFFG-IGF-1, MSC were incubated with MEM-α-medium, medium containing NapFFG, NapFFG-NO or NapFFG-1, under normal (standard cell culture) as well as under ischemic conditions (addition of H_2O_2). The expression of SDF-1 was determined by qRT-PCR.

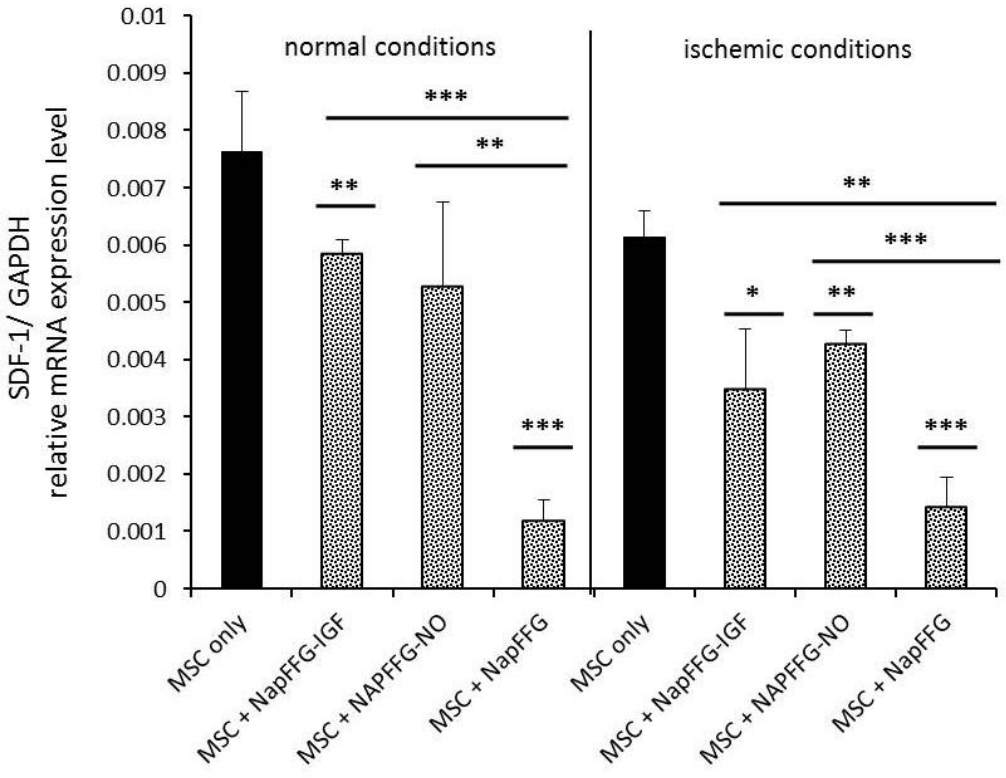

Fig.10: Relative expression level of SDF-1 in MSC. SDF-1 mRNA expression levels were determined by qRT-PCR in MSC cultured for 24h in MEM-α-medium control, medium

containing NapFFG-IGF-1, NapFFG-NO or NapFFG under “normal” (standard cell culture) as well as under ischemic conditions as mimicked by the presence of H_2O_2. Relative expression levels of SDF-1 were calculated using the quantification cycle (Cq) that represents the number of cycles necessary to reach a threshold signal level and were normalized to GAPDH expression level. Data are mean + SD (n=3, *** p <0.001, ** p <0.01, * p <0.05).

Under normal conditions (standard cell culture) no significant difference in the relative SDF-1 mRNA expression level between MSC in the control group (MSC only; 0.0076 ±0.001) and MSC treated with NapFFG-NO (0.0053 ±0.001) (Fig. 10) was determined. However, the relative SDF-1 expression in MSC treated with NapFFG-IGF-1 (0.0059 ±0.0002) and in MSC treated with NapFFG (0.0012 ±0.0004) was significantly lower than in the MSC control group.

Under ischemic conditions there was a significant difference in the relative SDF-1 mRNA expression levels between the MSC control group (MSC only; 0.0061 ±0.0004) and MSC treated with NapFFG-IGF-1 (0.0035 ±0.001). In the NapFFG-NO treated group the relative SDF-1 mRNA expression level (0.0043 ± 0.0002) was significantly lower than that in the MSC control group. Also in the NapFFG treated group the relative SDF-1 mRNA expression level of 0.0014 ±0.0005 was significantly lower than that in the MSC control group.

However, under normal conditions as well as under ischemic conditions, the relative SDF-1 mRNA expression level of MSC treated with NapFFG-IGF-1 or NapFFG-NO exhibited both a significant higher relative expression of SDF-1 as compared to that of MSC treated with NapFFG.

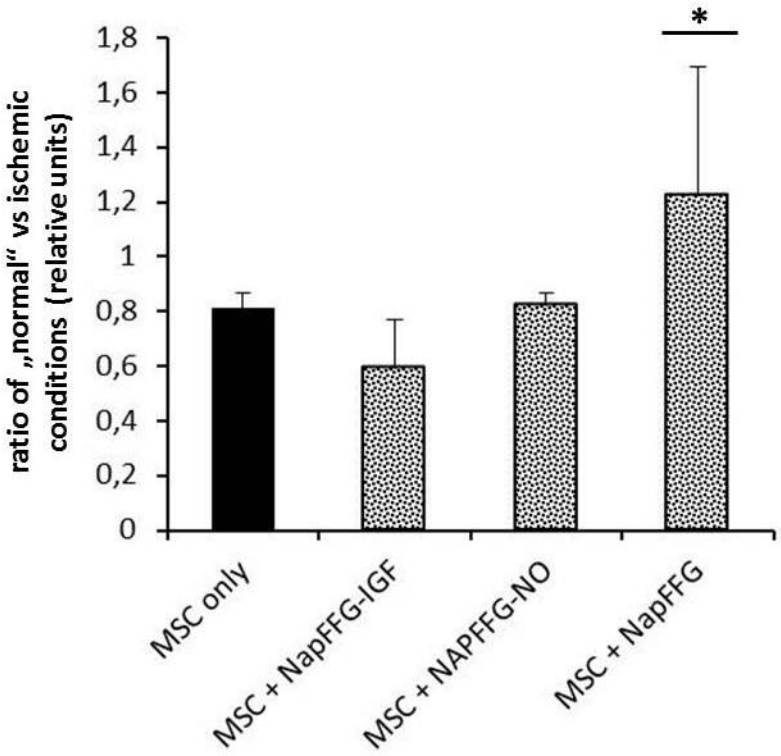

Fig.11: SDF-1 mRNA expression level in MSC upon treatment. SDF-1 mRNA expression levels were determined by qRT-PCR in MSC cultured for 24h in MEM-α-medium(MSC only), medium containing NapFFG-IGF-1, NapFFG-NO or NapFFG, under normal (standard cell culture) as well as under ischemic conditions as mimicked with H_2O_2. The ddCt was calculated using GAPDH expression as a control and the ratio between of untreated and treated cells termed as “normal” and ischemic conditions was calculated. Data are mean + SD (n=3, * p <0.05).

In comparison to the MSC control group (0.808 ±0.059), the ratio ddCt of NapFFG treated cells under “normal” vs ischemic conditions was significantly higher (1.227 ±0.469). In contrast, there was no significant effect of NapFFG-NO (0.824 ±0.044) or NapFFG-IGF-1 treatment (0.594 ±0.178) in the ratio of normal/ ischemic conditions (Fig. 11).

3.5 Effects of a Nitric Oxide-Releasing-Hydrogel on Cell Survival in a Mouse Model

The cell survival of MSC in mice was determined via the cells' luminescence signal in media, upon injection of NapFFG-hydrogel and NO-releasing hydrogel into the infarcted hearts (Fig. 12, Fig. 13).

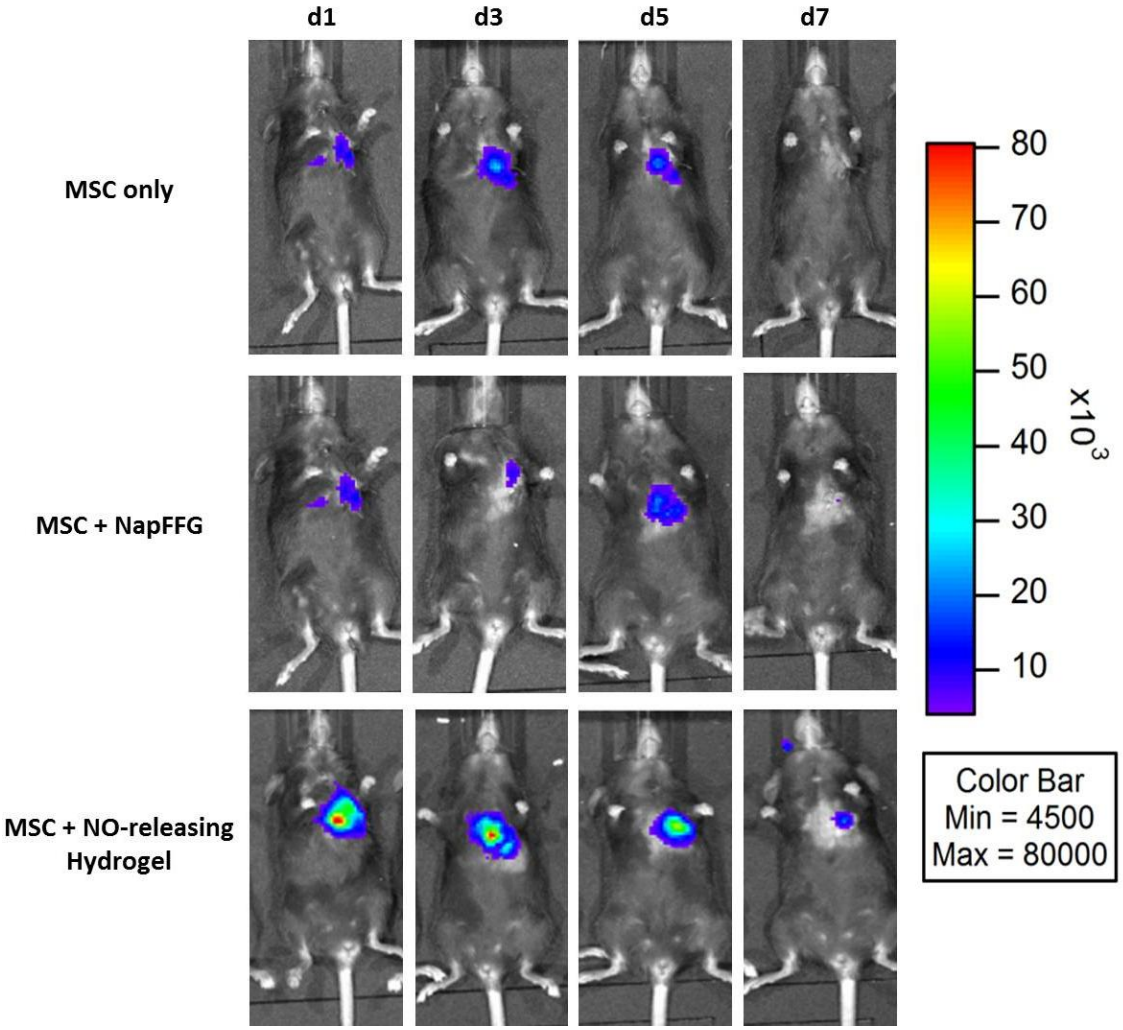

Fig.12: Luminescence signal of MSC in C57 mice. The luminescence signal was detected at day 1, 3, 5 and 7 after infarction and injection of MSC in media (MSC only), MSC in NapFFG-hydrogel and MSC in NO-releasing hydrogel. Mice received an injection of the substrate and the luminescence signal was detected during a 5min exposure time.

MSC injected in media alone (MSC only = control) showed a very weak luminescence signal 24h after injection in the infarcted heart. The signal increased until day 3 after the injection but decreased again until day 5 and was not visible on day 7 post injection of the cells.

The MSC signal 24h after the injection of the NapFFG-hydrogel was similarly weak as the signal of MSC injected in media (MSC only) and further decreased until day 3 after injection. Five days after injection the cells' luminescence signal increased but disappeared until day 7 as compared to the signal after 1day of injection.

The NO-releasing-hydrogel apparently improved cell viability *in vivo*, since the luminescence signal 24h after the injection was much higher than that of control treated mice (MSC only). Also after 3, 5 and 7 days of injection the intensities were higher as compared to that of control treated mice. Yet, the signal of MSC injected in the NO-releasing hydrogel declined over the period of 7 days (Fig. 12).

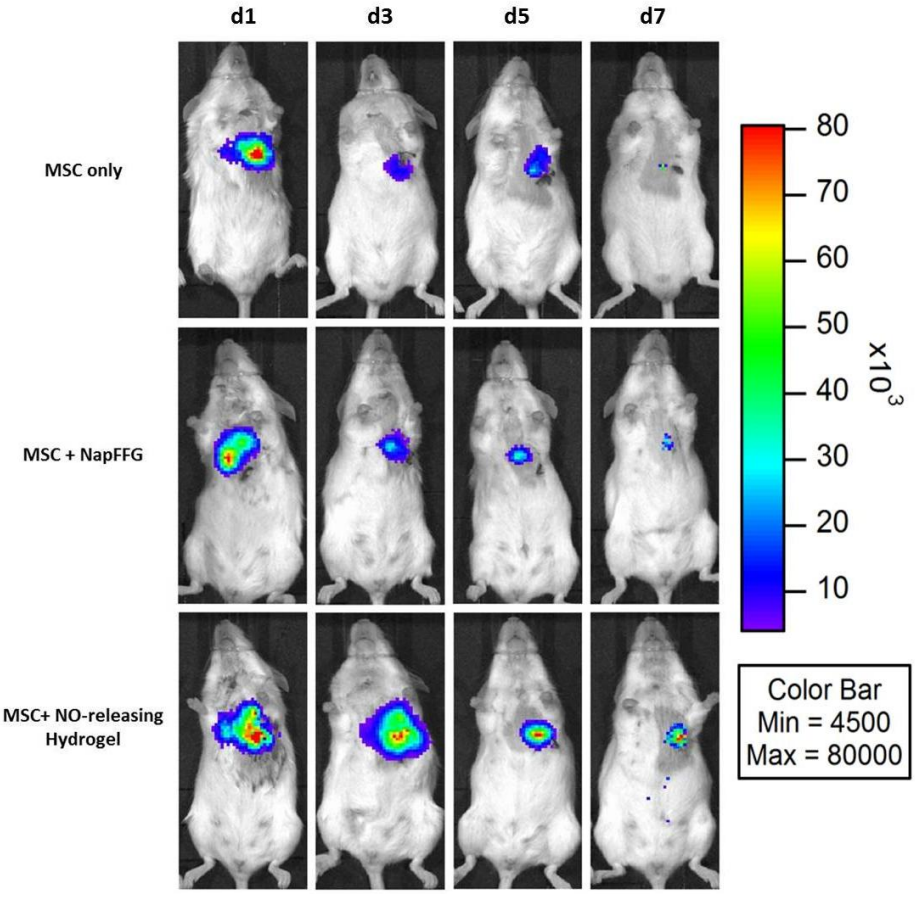

Fig.13: Luminescence signal of MSC in FVB mice. The luminescence signal was detected at day 1, 3, 5 and 7 after infarction and injection of MSC in media (MSC only),

MSC in NapFFG-hydrogel and MSC in NO-releasing hydrogel. Mice received an injection of the substrate and the luminescence signal was detected during a 5min exposure time.

Similar to C57 mice, treatment of FVB mice with MSC in media (MSC only) resulted in a low luminescence signal in the infarcted heart 24h after injection. The signal lost intensity every day until it disappeared on day 7 after the injection of the cells.

The intensity of the cell signal 24h after the injection of NapFFG-hydrogel was similarly low as the signal of MSC in media (MSC only), but was higher 3 days after the injection. Five days after the injection the intensity of the cells' luminescence signal decreased and the signal was barely visible on day 7.

The NO-releasing-hydrogel apparently improved the cell viability *in vivo*, since the luminescence signal's intensity 24h after the injection was higher than in mice which received MSC only and MSC in NapFFG-hydrogel. Also 3 days after the injection the signal's intensity was similarly high, but declined until day 5. However, the cells' luminescence signal was still more intense than that of MSC only and MSC in NapFFG-hydrogel. Seven days after the injection signal's intensities decreased in MSCs of all treatment groups, but that of MSC in the NO-releasing hydrogel remained highest (Fig. 13).

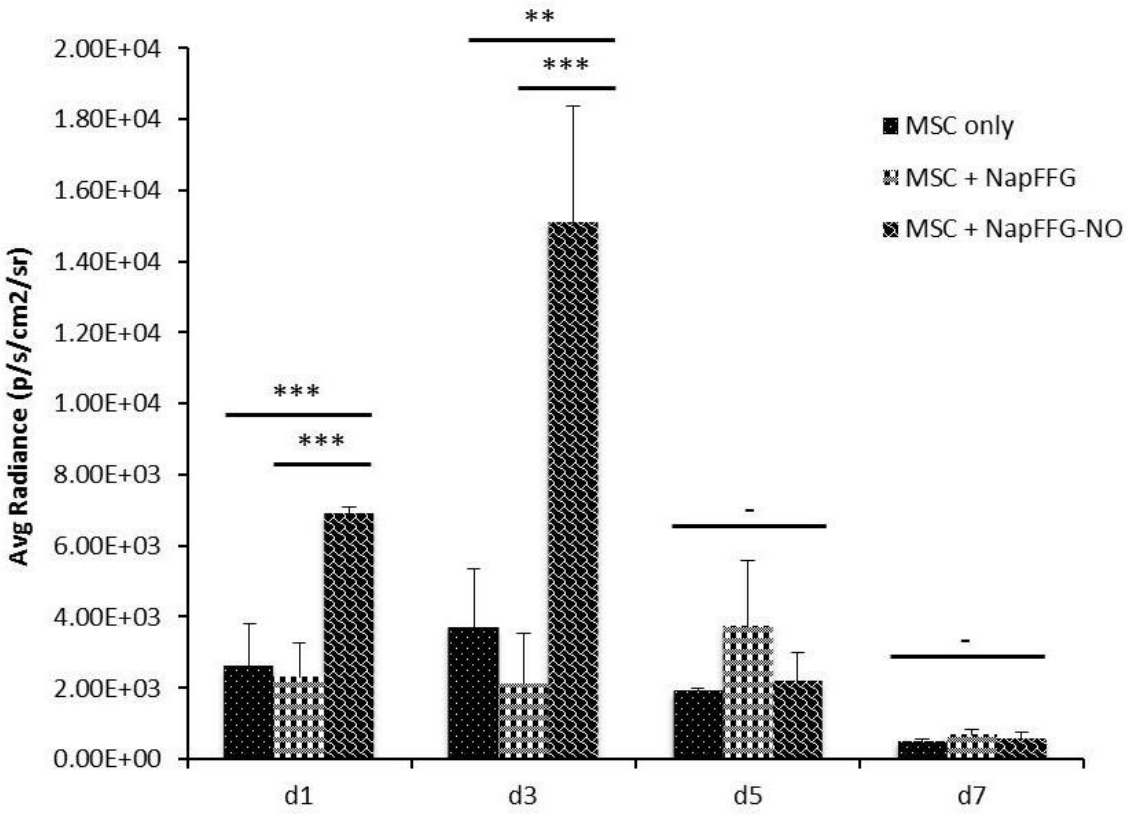

Fig.14: Luminescence signal of MSC in mice. The luminescence signal was detected by molecular imaging at day 1, 3, 5 and 7 after infarction and injection of MSC in media (MSC only), MSC in NapFFG-hydrogel and MSC in NO-releasing hydrogel in the infarcted heart. The figure shows the average of photons per second per square centimeter per steradian after 5min exposure time. Data are mean + SD (n=5, *** p <0.001, ** p <0.01, - p >0.05).

According to the molecular images, the luminescence signals of MSC only ($2.6x10^3$ $p/s/cm^2/sr$ ±1191.5) and MSC in NapFFG-hydrogel ($2.3x10^3$ $p/s/cm^2/sr$ ±982.03) 24h after the injections were significantly lower than that of MSC in NO-releasing hydrogel ($6.91x10^3$ $p/s/cm^2/sr$ ±202.53).

Three days after injection the number of MSC in NO-releasing hydrogel and therefore the luminescence signal in the mice increased significantly ($1.51x10^4$ $p/s/cm^2/sr$ ±3266.83) in comparison to MSC only ($3.71x10^3$ $p/s/cm^2/sr$ ±1631.36) and MSC in NapFFG-hydrogel ($2.12x10^3$ $p/s/cm^2/sr$ ±1422.93).

After 5 days there was no significant difference in the signal intensity of MSC only ($1.9x10^3$ p/s/cm^2/sr ±89.1), MSC in NapFFG-hydrogel ($3.72x10^3$ p/s/cm^2/sr ±1886.83) and MSC in the NO-releasing hydrogel ($2.2x10^3$ p/s/cm^2/sr ±812.71).

Moreover, 7 days after injection of MSC in the infarcted area there was also no significant difference in the luminescence signal of the different groups. "MSC only" led to a signal of $5.07x10^2$ p/s/cm^2/sr ±69.91, MSC in NapFFG-hydrogel a signal of $6.91x10^2$ p/s/cm^2/sr ±139.67 and MSC in NO-releasing hydrogel a signal of $5.67x10^2$ p/s/cm^2/sr ±199.92 (Fig. 14).

3.6 Impact of a Nitric Oxide-releasing-hydrogel on the Infarct Size in a Mouse Model

The hearts of mice were stained for Hematoxylin Eosin and Masson's Trichrome (Fig. 15, Fig. 17) to evaluate the infarction size in the left ventricle (Fig.16, Fig.18) and any effect of nitric oxide on the ischemic tissue regeneration (Fig. 19).

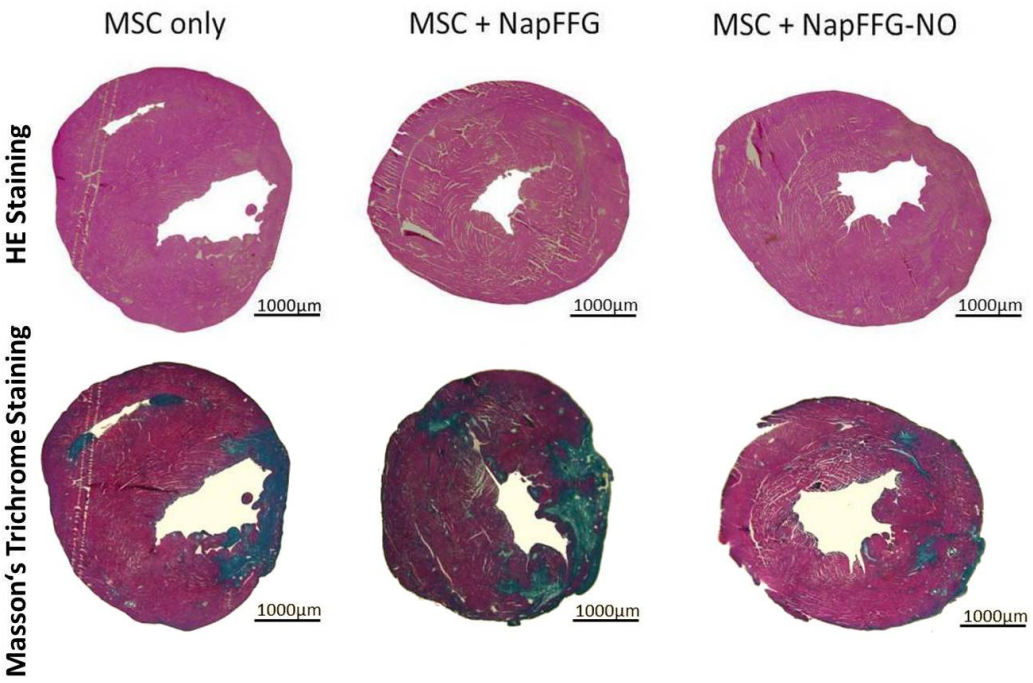

Fig. 15: Cross-sections of HE and Masson's Trichrome stained hearts. Mice were sacrificed 1 week after infarction and injection of MSC in saline (MSC only), MSC in

NapFFG-hydrogel or MSC in NO-releasing hydrogel. Then, tissue sections were HE and Masson's Trichrome stained and pictures taken at 2,5x magnification.

In the HE stained slides the muscle appeared in pink while the infarcted area showed a grey beige colour. Masson's Trichrome staining resulted in the visualization of the dark red muscle fibers and the greenish blue collagen deposit.

In mice which received MSC in NapFFG-hydrogel the infarcted area, 1 week after permanent ligation of the left descending coronary artery and injection of the cells, appeared bigger than in mice which received the MSC only treatment; as evident by a smaller blue area. Furthermore, the collagen deposit in the hearts of mice which received MSC in NO-releasing hydrogel appeared smaller than in mice which received the MSC control treatments (MSC only and MSC NapFFG) (Fig. 15).

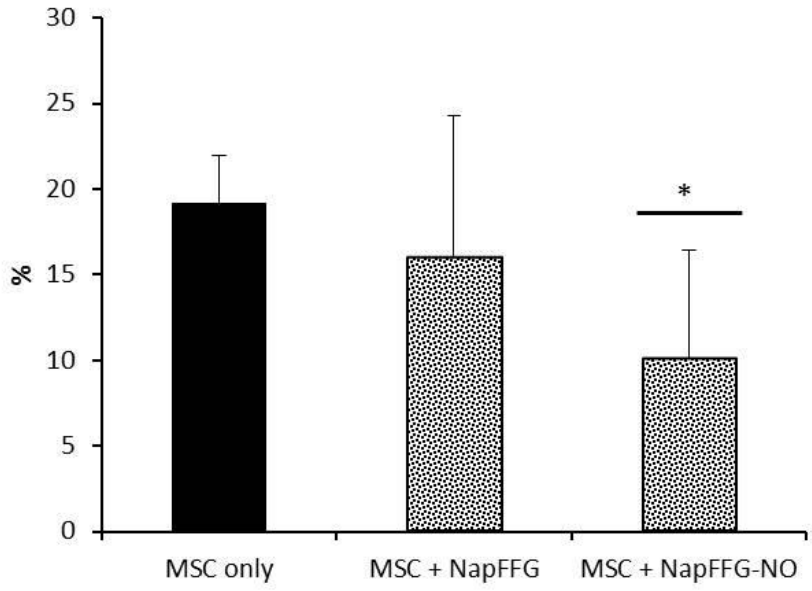

Fig. 16: Percentage of the infarcted area in the left ventricle after seven days of myocardial infarction. The infarct size was calculated by the size of the collagen area compared to the size of the left ventricle using stained hearts of mice, sacrificed 7 days after permanent ligation of the left descending coronary artery and injection of MSC in

saline (MSC only = control), NapFFG-hydrogel or a NO-releasing hydrogel. Data are mean + SD (n=5, * p <0.05).

One week after permanent ligation of the left descending coronary artery, the infarcted area in the heart of mice which received MSC only treatment (control) constituted 19.19% ±2.8 of the left ventricle. Mice which received MSC in NapFFG-hydrogel showed an infarcted area of 16.02% ±8.27 of the left ventricle whereas MSC in the NO-releasing hydrogel showed a significantly decreased infarct size of 10.09% ±6.37 of the left ventricle (Fig. 16).

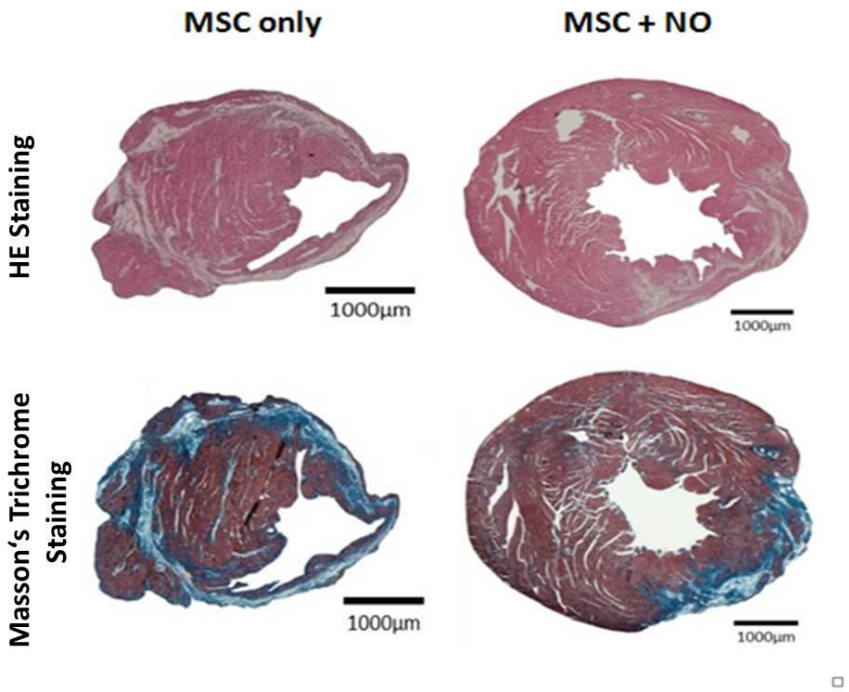

Fig. 17: Cross-sections of HE and Masson's Trichrome stained hearts. Mice were sacrificed 1 month after infarction and injection of MSC in saline (MSC only), MSC in NapFFG-hydrogel or MSC in NO-releasing hydrogel. Then, tissue sections were HE and Masson's Trichrome stained and pictures taken at 2,5x magnification.

In the HE stained slides the muscle appeared in pink while the infarcted area is colored in grey beige. After Masson's Trichrome staining muscle fibers displayed in a dark red and collagen deposit in a greenish blue.

In mice which received MSC in the NO-releasing hydrogel, 1 month after permanent ligation of the left descending coronary artery and injection of the cells, the collagen area appeared smaller than in mice which received the MSC in saline (Fig. 17).

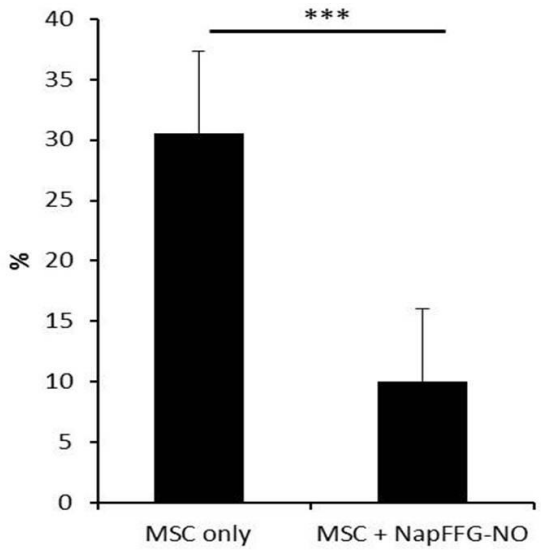

Fig. 18: Percentage of the infarcted area in the left ventricle one month after myocardial infarction. The infarct size was calculated by the size of the collagen area compared to the size of the left ventricle using stained hearts of mice, sacrificed 1 month after permanent ligation of the left descending coronary artery and which had received either injections of MSC in saline (MSC only control) or in a NO-releasing hydrogel. Data are mean + SD (n=5, *** p <0.001).

One month after permanent ligation of the left descending coronary artery, the infarcted area in the heart of mice which received MSC in saline (MSC only = control) was 30.51% ±6.78 of the left ventricle. Mice which received MSC in the NO-releasing hydrogel showed a significantly smaller infarcted area of 10.01% ±6.04 of the left ventricle (Fig. 18).

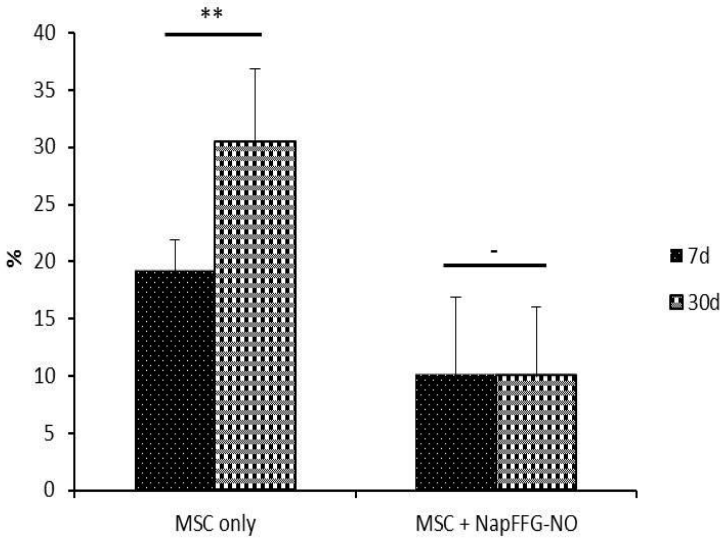

Fig. 19: Percentage of the infarcted area in the left ventricle one week and one month after myocardial infarction. The infarct size was calculated using the stained hearts of mice, sacrificed one week and one month after permanent ligation of the left descending coronary artery and injection of MSC in saline (MSC only =control) or in a NO-releasing hydrogel. Data are mean + SD (n=5, ** p <0.01, - p >0.05).

Mice, which received an injection of MSC in saline, were sacrificed seven days after permanent ligation of the left descending coronary artery, showed an infarcted area of 19.20% ±2.8 of the left ventricle. These mice showed a significant smaller collagen deposit as compared to mice which received the same treatment but were sacrificed after 30 days (30.51% ±6.78). Therefore, the infarct size increased significantly for 11.31% despite the MSC treatment (Fig. 19).

Mice, which were sacrificed seven days after permanent ligation of the left descending coronary artery and received an injection of MSC in NO-releasing hydrogel, showed an

infarcted area of 10.10% ±6.37 of the left ventricle. Mice which received the same treatment but were sacrificed after 30 days also showed a collagen deposit of 10.01% ±6.04 of the left ventricle. Consequently, in mice which received MSC in a NO-releasing hydrogel the infarct size remained unchanged (Fig. 19) since the hydrogel affected both the MSC and the ischemic tissue.

4. Discussion

Research has recently focused on stem cell-based treatments of myocardial infarction. MSCs display many desirable qualities for the treatment of ischemic tissue, but their sensitivity to the hypoxic and inflammatory environment is problematic [29][49]. Studies have demonstrated poor survival of transplanted cells *in vivo*, resulting in limited tissue regeneration due to cell death [50]. In recent years studies have focused on the modification of the cells through heat shock, hypoxia preconditioning or genetic transfection [51]. In fact, improved cell survival via hypoxia preconditioning has been reported [26][29]. Additionally, various biomaterials, like fibrin glue, collagen matrices and self-assembling peptide nanofibers have been used to transplant cells into the damaged myocardium to improve their survival [52]. This study focused on the construction of an extracellular environment to improve the survival of stem cells and consequently the tissue repair capacity in a transplantation study.

A glycosylated nitric oxide donor was conjugated to NapFFG, a polymer with hydrophilic property, to form a NO-releasing hydrogel. The release of NO was controlled by the enzymatic activity of ß-Galactosidase, which breaks the glucosidic bond to the donor protective galactose and triggers the NO release. The NO release is controlled by the concentration of the enzyme. Furthermore, the conjugation of the donor to the gel forming compound NapFFG reduces the possibility of NO accumulation and burst release [48][53]. The possibility to control the NO release is an important fact, since high concentrations of NO are known to be toxic [32] [35] [37].

To improve cell survival and cardioprotective effect of stem cell therapy, a second hydrogel was synthesized for a possible therapeutic use *in vivo*. IGF-1 mediated signaling results in regulation of cell growth and proliferation, cell survival and motility. [41] Therefore an IGF-1 active site linked NapFFG hydrogel was synthesized.

Additives on a NapFFG-hydrogel and the NapFFG-hydrogel itself were carefully tested for their proliferative effects on MSC as well as on a possible angiogenic and anti-inflammatory potential. Furthermore, the effect of a NO releasing hydrogel on both the survival of MSC in a mouse model of myocardial infarction and the effect on the infarct size were determined.

The NapFFG-hydrogel itself showed a minor negative effect on the proliferation of MSC *in vitro*. This may indicate cyto-toxicity of the NapFFG compound. However, a NO releasing hydrogel markedly increased the proliferation of MSC. Several studies have already described an enhanced viability and proliferation of endothelial cells (EC), while Murohara *et al.* suggest that NO might be more critical in endothelial migration than in proliferation [15][53-54]. This growth promoting effect on EC is associated with cGMP generation and PKG activity for MAPK cascades Ras, Raf, and ERK1/2 signaling activation [1].

The construct of an IGF-1 active site hydrogel revealed increased proliferation of MSC after 48h of injection, while the cell growth decreased again after 72h. This negative effect on cell growth might be caused by the toxicity of the NapFFG gel forming compound rather than by IGF-1 itself. However, IGF-1 is known to increase cell proliferation in various cell types. This might be mediated by the stimulation of DNA synthesis through IGF-1, which is acting as progression factor [55] and by Akt-mediated signaling [40]. Correspondingly, Kofidis *et al.* reported increased proliferation and mitogenesis in myocytes [8]. Furthermore, the proliferation of myoblasts by MAPK pathway [20] as well as an IGF/PI3-kinase/Akt signaling-mediated increased proliferation of cardiomyocytes derived from human embryonic stem cells [56] was already demonstrated.

The vascular endothelial growth factor (VEGF) is a potent angiogenic factor, which plays a critical role in both, physiological and pathological angiogenesis [1][57-59]. Furthermore, VEGF is responsible for stem cell recruitment to the ischemic tissue [60] and confers cardio protection by activation of the reperfusion injury salvage kinase (RISK) pathway such as PI3K-Akt-eNOS or MEK1/2-Erk1/2-p90rsk [58]. Therefore, in this study a possible angiogenic potential of the hydrogel on MSC was investigated by the expression of the angiogenic factor VEGF. Furthermore, NO has been described to trigger VEGF induced angiogenesis. Several studies suggest that NO modulates VEGF-induced angiogenesis under pathological processes [11][34][57]. Therefore, NO might be an important modulator of VEGF synthesis in physiological as well as in pathological processes [34]. A lack of NO results in reduced angiogenesis [57] which suggests that NO might be an important angiogenesis inducing factor. Luczak *et al.* found that NO

induces angiogenesis via ETS-1 expression [36], while Murohara *et al.* reported that NO inhibits angiogenesis [15]. Additionally, Murohara *et al.* described endothelial derived NO as a mediator for angiogenesis *in vitro* and *in vivo* [15].

In our study, we investigated the effect of NO on expression levels of VEGF in MSC under both physiological and ischemic conditions. We found that NapFFG-NO decreased the expression of VEGF in MSC. The discrepancies in the described down-regulation of VEGF might be due to the conjugation of the NO donor on the toxic NapFFG. Hence, compared to the low VEGF expression in MSC with NapFFG control, the VEGF expression in MSC in the presence of NO was significantly higher. Thus, NapFFG-NO induced VEGF expression in MSC compared to the NapFFG control.

IGF-1 has been reported to increase the level of proangiogenic factors like VEGF and TGF-ß after myocardial infarction and might induce angiogenesis [14]. Zhu *et al.* demonstrated an increased VEGF-C expression via the PI3K/Akt and MAPK/ERK1/2 signaling pathways in breast cancer cells [61]. Upregulation of VEGF was also shown in a HIF1α-mediated way: IGF-1 increased HIF1α protein levels and VEGF transcription in embryonic stem cells [20].

In the present study IGF-1 showed an increased relative VEGF expression level in MSC compared to NapFFG treated cells under ischemic conditions. Yet, compared to the non-treated control VEGF expression level were not different, neither under “normal” (standard cell culture) nor under ischemic conditions. Again these discrepancies in the angiogenic potential could be explained by the conjugation of the IGF-1 active site to the toxic NapFFG. In fact, the ratio of the VEGF expression in the presence of the IGF-1 active site hydrogel revealed a significant increase.

Repair of ischemic tissue and ventricular remodeling in the infarcted heart requires the suppression of inflammatory processes [5]. NO has been demonstrated to have anti-inflammatory effects [35]. Accordingly, Smith *et al.* reported decreased expression levels of the immune modulatory cytokine TGF-ß via NO after eNOS gene transfer [3]. In contrast, eNOS overexpression in cardiac tissues also increased the expression of the inflammatory cytokine SDF-1 [62]. NO was also shown to reduce inflammatory responses (inhibition of TGF-ß and NF-kappaB activation) by mediating tissue kallikrein

[5]. Additionally, IGF-1 has been also described to reduce inflammatory processes and oxidative stress. It was shown to down-regulate the expression of vascular pro-inflammatory cytokines like TNF-α and IL-6 [63]. Furthermore, patients with low IGF-1 levels showed a higher association to inflammation and an increased mortality in cardiovascular diseases [64].

The stroma cell derived factor 1 (SDF-1), also known as CXC motif ligand 12 (CXCL-12), is a cell recruiting cytokine binding to the CXC receptor 4 (CXCR-4). Its synthesis is induced in response to inflammatory and immunological processes. SDF-1 is a chemo-attractant of EC, which implies that SDF-1 is an important protein in re-endothelialisation and stem cell recruitment after vascular injury [62][65-66].

In our hands IGF-1 and NapFFG treated cells revealed a decreased expression of SDF-1 in MSCs under “normal” (standard cell culture) conditions *in vitro*. Under ischemic conditions, IGF-1, NapFFG as well as NO treated cells showed a decreased relative SDF-1 expression level as compared to the control group, but NapFFG treated MSCs showed a higher ratio in the expression under “normal” and ischemic conditions. This suggests that the environment does not trigger an inflammatory response *in vitro*. On the other hand SDF-1 is essential for the stem cell homing to the ischemic tissue [65-67]. Therefore, MSCs upon hydrogel treatment might not be that efficient in stem cell recruitment and inducing protective processes, since SDF-1 is known to conduct multiple protective effects such as anti-apoptosis, pro-survival, endothelial progenitor cells recruitment and neo-vascularization or to improve cardiac function [62][67].

In myocardial ischemia, MSC transplantation is expected to provide a renewable source of proliferating and functional cells and, simultaneously, to trigger cell differentiation and neovascularization by the release of paracrine factors [7][21][28-29]. Therefore, several studies reported an improvement of the heart function, decreased infarct size and decreased mortality rate after MSC transplantation [7][28-29]. Furthermore, injection of MSC has been shown to improve regeneration of patients with myocardial ischemia [40][68].

IGF-1 treatment offers a promising approach in ischemic tissue regeneration, since IGF-1 levels are critical in the recovery of ischemic cardiomyopathy and in the reduction of

ischemia-reperfusion damage. IGF-1 is known to act via decreasing apoptosis and inflammation through interaction with IGF-1R on EC and cardiomyocytes. Furthermore, patients suffering from myocardial ischemia show significantly lower IGF-1 levels. [40]. IGF-1 was also shown to reduce ischemia and to increase pro-angiogenic factors in rats with myocardial infarction [14].

Nitric oxide is used for the treatment of myocardial infarction, since it's known to have inductive effects on BMSCs and to initiate phenotypic changes in the differentiation of cardiomyocytes [33]. Several groups reported a decreased infarction size and an improved cardiac function by nitric oxide generation [51][69-71]. NO inhalation [72], a NO-donor [35][71] or eNOS gene therapy led to inhibition of cardiomyocyte apoptosis, suppression of oxidative stress and promotion of angiogenesis [3][11][73]. On the contrary, high concentrations of NO depressed cardiomyocytes function and induce inflammatory processes and cell death [71].

In line with these findings our study indicates that a NO-releasing hydrogel improves the survival of MSC in a transplantation study and, additionally, decreases the infarct size as compared to control MSC treated animals. This might be due to combined long-term effect on both the MSC and the ischemic tissue.

These findings are in line with that reported by Liu *et al*., who showed that a chitosan hydrogel not only improved the survival of transplanted stem cells but also the heart function after myocardial infarction [74].

5. Conclusion and Future Perspectives

The nitric oxide releasing hydrogel as well as the IGF-1 active site hydrogel might be valuable in a variety of therapeutic approaches in regenerative medicine. This is based on the observation that the hydrogel with additives did not generate an inflammatory environment for cells, and the nitric oxide releasing hydrogel as well as the IGF-1 active site hydrogel did not increase MSCs angiogenic potential. Furthermore, the NO-releasing hydrogel improved cell proliferation *in vitro* and survival *in vivo* and decreased the infarct size in a mouse model. Therefore, it represents an effective injectable scaffold and cell carrier with therapeutic effects on both the transplanted cells and the ischemic myocardium.

The loss of cells after injection still remains a challenge for a stem cell-based therapy of myocardial infarction. Especially the toxicity of the gel forming compound NapFFG needs further investigations to improve the cell survival and the regeneration of the ischemic tissue. Furthermore, the injection of MSC in the IGF-1 active site hydrogel was impossible, due to loss of the gel consistency. Consequently, the gel forming capacity should be improved to provide an effective injectable scaffold for further studies.

Generally, published studies including animal models and human studies suggest that MSC based cell therapy may offer a safe, feasible and effective treatment after myocardial infarction due to their therapeutic potential. Based on literature and our data we conclude that a combination of both, stem cells and promoting factors in a hydrogel, might provide a valid tool for tissue regeneration after myocardial infarction. Future studies are needed to test additional promoting factor and cell carrier material for a more optimized cell-based therapy option of myocardial infarction.

6. References

[1] S. C. Bir, Y. Xiong, C. G. Kevil, and J. Luo, “Emerging role of PKA/eNOS pathway in therapeutic angiogenesis for ischaemic tissue diseases.,” *Cardiovascular research*, vol. 95, no. 1, pp. 7–18, Jul. 2012.

[2] Z. Cheng, L. Ou, Y. Liu, X. Liu, F. Li, B. Sun, Y. Che, D. Kong, Y. Yu, and G. Steinhoff, “Granulocyte colony-stimulating factor exacerbates cardiac fibrosis after myocardial infarction in a rat model of permanent occlusion.,” *Cardiovascular research*, vol. 80, no. 3, pp. 425–34, Dec. 2008.

[3] R. J. Smith, J. Agata, C. Xia, L. Chao, and J. C. T, “Human endothelial nitric oxide synthase gene delivery protects against cardiac remodeling and reduces oxidative stress after myocardial infarction,” *Life Sciences*, vol. 76, pp. 2457–2471, 2005.

[4] K. Thygesen, J. S. Alpert, A. S. Jaffe, M. L. Simoons, B. R. Chaitman, H. D. White, H. a Katus, F. S. Apple, B. Lindahl, D. a Morrow, B. a Chaitman, P. M. Clemmensen, P. Johanson, H. Hod, R. Underwood, J. J. Bax, R. O. Bonow, F. Pinto, R. J. Gibbons, K. a Fox, D. Atar, L. K. Newby, M. Galvani, C. W. Hamm, B. F. Uretsky, P. G. Steg, W. Wijns, J.-P. Bassand, P. Menasché, J. Ravkilde, E. M. Ohman, E. M. Antman, L. C. Wallentin, P. W. Armstrong, J. L. Januzzi, M. S. Nieminen, M. Gheorghiade, G. Filippatos, R. V Luepker, S. P. Fortmann, W. D. Rosamond, D. Levy, D. Wood, S. C. Smith, D. Hu, J.-L. Lopez-Sendon, R. M. Robertson, D. Weaver, M. Tendera, A. a Bove, A. N. Parkhomenko, E. J. Vasilieva, and S. Mendis, “Third universal definition of myocardial infarction.,” *European heart journal*, vol. 33, no. 20, pp. 2551–67, Oct. 2012.

[5] H. Yin, L. Chao, and J. Chao, “Nitric oxide mediates cardiac protection of tissue kallikrein by reducing inflammation and ventricular remodeling after myocardial ischemia / reperfusion,” *Life Sciences*, vol. 82, pp. 156–165, 2008.

[6] L. Barile, M. Gherghiceanu, M. Popescu, T. Moccetti, and G. Vassalli, “Human Cardiospheres as a Source of Multipotent Stem and Progenitor Cells,” *Stem Cells International*, vol. 2013, 2013.

[7] M. Elnakish, F. Hassan, D. Dakhlallah, C. Marsh, I. Alhaider, and M. Khan, “Mesenchymal stem cells for cardiac regeneration: Translation to bedside reality,” *Stem Cells International*, vol. 2012, Jan. 2012.

[8] T. Kofidis, J. L. De Bruin, T. Yamane, L. B. Balsam, D. R. Lebl, R. Swijnenburg, M. Tanaka, I. L. Weissman, and C. Robbins, “Insulin-Like Growth Factor Promotes Engraftment, Differentiation, and Functional Improvement after Transfer of Embryonic Stem Cells for Myocardial Restoration,” *Stem Cells*, vol. 22, pp. 1239–1245, 2004.

[9] L. E. Paulis, A. M. Klein, A. Ghanem, T. Geelen, B. F. Coolen, M. Breitbach, K. Zimmermann, K. Nicolay, B. K. Fleischmann, W. Roell, and G. J. Strijkers, “Embryonic Cardiomyocyte , but Not Autologous Stem Cell Transplantation , Restricts Infarct Expansion , Enhances Ventricular Function , and Improves Long-Term Survival,” *PloS one*, vol. 8, no. 4, 2013.

[10] D. Angoulvant, S. Fazel, and R. Li, “Neovascularization derived from cell transplantation in ischemic myocardium Introduction : Ischemic cardiomyopathy,” *Molecular and cellular biochemistry*, vol. 4, pp. 133–142, 2004.

[11] J. Li, Y. Zhang, C. Li, J. Xie, Y. Liu, W. Zhu, X. Zhang, S. Jiang, L. Liu, and D. Zhengnian, “HSPA12B Attenuates Cardiac Dysfunction and Remodeling after Myocardial Infarction through an eNOS-dependent Mechanism,” *Cardiovasc Res.*, vol. 99, no. 4, pp. 674–684, 2013.

[12] A. S. Chung and N. Ferrara, “The Extracellular Matrix & Angiogenesis: Role of the Extracellular Matrix in Developin Vessels and Tumor Angiogenesis.” Pathways Issue 11, San Francisco, 2010.

[13] M. Kubo, T.-S. Li, H. Kurazumi, Y. Takemoto, M. Ohshima, Y. Yamamoto, A. Nishimoto, A. Mikamo, M. Fujimoto, A. Nakai, and K. Hamano, “Heat shock factor 1 contributes to ischemia-induced angiogenesis by regulating the mobilization and recruitment of bone marrow stem/progenitor cells.,” *PloS one*, vol. 7, no. 5, Jan. 2012.

[14] M. Lisa, N. Haleagrahara, and S. Chakravarthi, “Insulin-Like Growth Factor-1 (IGF-1) Reduces ischemic changes and increases circulating angiogenic factors in experimentally - induced myocardial infarction in rats.,” *Vascular cell*, vol. 3, no. 1, Jan. 2011.

[15] T. Murohara, B. Witzenbichler, I. Spyridopoulos, T. Asahara, A. Sullivan, D. W. Losordo, J. M. Isner, E. C. Migration, and B. Ding, “Role of Endothelial Nitric Oxide Synthase in Endothelial Cell Migration,” *Arterioscler Thromb Vasc Biol.*, vol. 19, pp. 1156–1161, 1999.

[16] W. J. M. Mulder and A. W. Griffioen, “Imaging of angiogenesis.,” *Angiogenesis*, vol. 13, no. 2, pp. 71–4, Jun. 2010.

[17] S. Amadesi, C. Reni, R. Katare, and M. Meloni, “Role for Substance P-based Nociceptive Signaling in Progenitor Cell Activation and Angiogenesis Durin Ischemia in Mice and in Human Subjects,” *Circulation*, vol. 125, no. 14, pp. 1774–19, 2012.

[18] P. C. Brooks, a M. Montgomery, M. Rosenfeld, R. a Reisfeld, T. Hu, G. Klier, and D. a Cheresh, “Integrin alpha v beta 3 antagonists promote tumor regression by inducing apoptosis of angiogenic blood vessels.,” *Cell*, vol. 79, no. 7, pp. 1157–64, Dec. 1994.

[19] P. Kruzliak, G. Kovacova, and O. Pechanova, “Therapeutic potential of nitric oxide donors in the prevention and treatment of angiogenesis-inhibitor-induced hypertension.,” *Angiogenesis*, vol. 16, no. 2, pp. 289–95, Apr. 2013.

[20] S. M. Piecewicz, A. Pandey, B. Roy, S. H. Xiang, B. R. Zetter, and S. Sengupta, “Insulin-like growth factors promote vasculogenesis in embryonic stem cells.,” *PloS one*, vol. 7, no. 2, Jan. 2012.

[21] E. M. Horwitz and W. R. Prather, “Cytokines as the Major Mechanism of Mesenchymal Stem Cell Clinical Activity : Expanding the Spectrum of Cell Therapy,” *IMAJ*, vol. 11, pp. 4–6, 2009.

[22] S. C. Bendall, M. H. Stewart, P. Menendez, D. George, K. Vijayaragavan, T. Werbowetski-Ogilvie, V. Ramos-Mejia, A. Rouleau, J. Yang, M. Bossé, G. Lajoie, and M. Bhatia, “IGF and FGF cooperatively establish the regulatory stem cell niche of pluripotent human cells in vitro.,” *Nature*, vol. 448, no. 7157, pp. 1015–21, Aug. 2007.

[23] K. G. Sylvester and M. T. Longaker, “Stem Cells,” *Arch Surg*, vol. 139, pp. 93–99, 2004.

[24] M. Al-Nbaheen, R. Vishnubalaji, D. Ali, A. Bouslimi, F. Al-Jassir, M. Megges, A. Prigione, J. Adjaye, M. Kassem, and A. Aldahmash, “Human stromal (mesenchymal) stem cells from bone marrow, adipose tissue and skin exhibit differences in molecular phenotype and differentiation potential.,” *Stem cell reviews*, vol. 9, no. 1, pp. 32–43, Feb. 2013.

[25] A. Liew and T. O. Brien, “Therapeutic potential for mesenchymal stem cell transplantation in critical limb ischemia,” *Stem Cell Research & therapy*, vol. 3, no. 28, 2012.

[26] I. Rosova, M. Dao, B. Capoccia, D. Link, and J. A. Nolta, “Hypoxic Preconditioning Results in Increased Motility and Improved Therapeutic Potential of Human Mesenchymal Stem Cells,” *Stem Cells*, vol. 26, no. 8, pp. 2173–2182, 2008.

[27] G. Chamberlain, J. Fox, B. Ashton, and J. Middleton, “Concise review: mesenchymal stem cells: their phenotype, differentiation capacity, immunological features, and potential for homing.,” *Stem cells (Dayton, Ohio)*, vol. 25, no. 11, pp. 2739–49, Nov. 2007.

[28] M. Gnecchi, P. Danieli, and E. Cervio, “Mesenchymal stem cell therapy for heart disease,” *Vascular Pharmacology*, vol. 57, no. 1, pp. 48–55, Aug. 2012.

[29] X. Hu, S. P. Yu, J. L. Fraser, Z. Lu, M. E. Ogle, J. Wang, and L. Wei, “Transplantation of hypoxia-preconditioned mesenchymal stem cells improves infarcted heart function via enhanced survival of implanted cells and angiogenesis,” *Journal of Thoracic and Cardiovascular Surgery*, vol. 145, no. 4, pp. 799–808, 2008.

[30] T. Kinnaird, E. Stabile, M. S. Burnett, C. W. Lee, S. Barr, S. Fuchs, and S. E. Epstein, “Marrow-Derived Stromal Cells Express Genes Encoding a Broad Sprectrum of Arteriogenic Cyotkines and Promote In Vitro and In Vivo Arteriogenesis Through Paracrine Mechanisms,” *Circulation*, vol. 94, pp. 678–685, 2004.

[31] T. Kinnaird, E. Stabile, M. . Burnett, M. Shou, C. . Lee, S. Barr, S. Fuchs, and S. . Eppstein, “Local Delivery of Marrow-Derived Stromal Cells Augments,” *Circulation*, vol. 109, pp. 1543–1549, 2004.

[32] S. M. Davidson and M. R. Duchen, “Effects of NO on mitochondrial function in cardiomyocytes : Pathophysiological relevance,” *Cardiovascular research*, vol. 71, pp. 10–21, 2006.

[33] J. W. Fuseler and M. T. Valarmathi, “Biomaterials Modulation of the migration and differentiation potential of adult bone marrow stromal stem cells by nitric oxide,” *Biomaterials*, vol. 33, no. 4, pp. 1032–1043, 2012.

[34] T. Namba, H. Koike, K. Murakami, A. Motokuni, H. Makino, N. Hashiya, T. Ogihara, Y. Kaneda, M. Kohno, and R. Morishita, “Angiogenesis Induced by Endothelial Nitric Oxide Synthase Gene Through Vascular Endothelial Growth Factor Expression in a Rat Hindlimb Ischemia Model,” *Circulation*, vol. 108, pp. 2250–2257, 2003.

[35] B. W. Roberts, J. Mitchell, J. H. Kilgannon, M. E. Chansky, and S. Trzeciak, “NITRIC OXIDE DONOR AGENTS FOR THE TREATMENT OF ISCHEMIA/

REPERFUSION INJURY IN HUMAN SUBJECTS: A SYSTEMATIC REVIEW," *SHOCK*, vol. 39, no. 3, pp. 229–239, 2013.

[36] K. Luczak, A. Balcerczyk, M. S. Ski, and G. Bartosz, "Low concentration of oxidant and nitric oxide donors stimulate proliferation of human endothelial cells in vitro," *Cell Biology International*, vol. 28, pp. 483–486, 2004.

[37] G. Heusch, K. Boengler, and R. Schulz, "Cardioprotection: Nitric Oxide, Protein Kinases and Mitochondria," *Circulation*, vol. 118, pp. 1915–1919, 2008.

[38] M. Annunziata, R. Granata, and E. Ghigo, "The IGF system.," *Acta diabetologica*, vol. 48, no. 1, pp. 1–9, Mar. 2011.

[39] I. Heidegger, A. Pircher, H. Klocker, and P. Massoner, "Targeting the insulin-like growth factor network in cancer therapy," *Cancer Biology & Therapy*, vol. 11, no. 8, pp. 701–707, Apr. 2011.

[40] E. Conti, M. B. Musumeci, G. E. Assenza, G. Quarta, C. Autore, and M. Volpe, "Recombinant human insulin-like growth factor-1: a new cardiovascular disease treatment option?," *Cardiovascular & hematological agents in medicinal chemistry*, vol. 6, no. 4, pp. 258–71, Oct. 2008.

[41] M. M. Chitnis, J. S. P. Yuen, A. S. Protheroe, M. Pollak, and V. M. Macaulay, "The type 1 insulin-like growth factor receptor pathway.," *Clin Cancer Res*, vol. 14, no. 20, pp. 6364–70, Oct. 2008.

[42] E. R. King and K.-K. Wong, "Insulin-like growth factor: current concepts and new developments in cancer therapy.," *Recent patents on anti-cancer drug discovery*, vol. 7, no. 1, pp. 14–30, Jan. 2012.

[43] R. Sarfstein and H. Werner, "Minireview: nuclear insulin and insulin-like growth factor-1 receptors: a novel paradigm in signal transduction.," *Endocrinology*, vol. 154, no. 5, pp. 1672–9, May 2013.

[44] K. Siddle, “Signalling by insulin and IGF receptors: supporting acts and new players.,” *Journal of molecular endocrinology*, vol. 47, pp. R1–R10, Aug. 2011.

[45] a. Juul, “Low Serum Insulin-Like Growth Factor I Is Associated With Increased Risk of Ischemic Heart Disease: A Population-Based Case-Control Study,” *Circulation*, vol. 106, no. 8, pp. 939–944, Aug. 2002.

[46] S. J. Weroha and P. Haluska, “IGF System in Cancer,” *Endocinol Metab Clin North Am*, vol. 41, no. 2, pp. 1–15, 2013.

[47] M. Jansen, F. van Schaik, A. . Ricker, B. Bullock, D. . Woods, K. . Gabbay, A. . Nussbaum, S. J.S, and V. den B. J.L, “Sequence of cDNA encoding human insulin-like growth factor I precursor,” *Nature*, vol. 306, no. 8, pp. 609–611, 1983.

[48] J. Gao, W. Zhang, J. Zhang, D. Guan, Z. Yang, D. Kong, and Q. Zhao, “Enzyme-controllable delivery of nitric oxide from a molecular hydrogel,” *Chem. Commun.*, vol. 49, pp. 9173–9175, 2013.

[49] L. Gao, G. Bledsoe, H. Yin, B. Shen, L. Chao, and J. Chao, “Tissue Kallikrein-Modified Mesenchymal Stem Cells Provide Enhanced Protection Against Ischemic Cardiac Injury After Myocardial Infarction,” *Circ J.*, vol. 77, no. 8, pp. 2134–2144, 2013.

[50] T. E. Robey, M. K. Saiget, H. Reinecke, and C. E. Murry, “Systems Approaches to Preventing Transplanted Cell Death in Cardiac Repair,” *J Mol Cell Cardiol*, vol. 45, no. 4, pp. 567–581, 2008.

[51] L. Song, Y. Yang, Q. Dong, H. Qian, R. Gao, S. Qiao, and R. Shen, “Atorvastatin Enhance Efficacy of Mesenchymal Stem Cells Treatment for Swine Myocardial Infarction via Activation of Nitric Oxide Synthase,” *PloS one*, vol. 8, no. 5, 2013.

[52] W. Dai, S. L. Hale, G. L. Kay, A. J. Jyrala, and R. A. Kloner, “Delivering stem cells to the heart in a collagen matrix reduces relocation of cells to other organs as assessed by nanoparticle technology,” *Regen Med*, vol. 4, no. 3, pp. 387–395, 2009.

[53] Q. Zhao, J. Zhang, L. Song, Q. Ji, Y. Yao, Y. Cui, and J. Shen, “Polysaccharide-based biomaterials with on-demand nitric oxide releasing property regulated by enzyme catalysis,” *Biomaterials*, vol. 34, no. 33, pp. 8450–8458, 2013.

[54] M. Kushwaha, J. M. Anderson, C. A. Bosworth, A. Andukuri, W. P. Minor, J. R. Lancaster, P. G. Anderson, B. C. Brott, and H. Jun, “Biomaterials A nitric oxide releasing , self assembled peptide amphiphile matrix that mimics native endothelium for coating implantable cardiovascular devices,” *Biomaterials*, vol. 31, no. 7, pp. 1502–1508, 2010.

[55] a J. Butt, S. M. Firth, and R. C. Baxter, “The IGF axis and programmed cell death.,” *Immunology and cell biology*, vol. 77, no. 3, pp. 256–62, Jun. 1999.

[56] T. C. McDevitt, M. a Laflamme, and C. E. Murry, “Proliferation of cardiomyocytes derived from human embryonic stem cells is mediated via the IGF/PI 3-kinase/Akt signaling pathway.,” *Journal of molecular and cellular cardiology*, vol. 39, no. 6, pp. 865–73, Dec. 2005.

[57] D. Fukumura, T. Gohongi, A. Kadambi, Y. Izumi, J. Ang, C. Yun, D. G. Buerk, P. L. Huang, and R. K. Jain, “Predominant role of endothelial nitric oxide synthase in vascular endothelial growth factor-induced angiogenesis and vascular permeability,” *PNAS*, vol. 98, no. 5, pp. 2604–2609, 2001.

[58] D. J. Hausenloy and D. M. Yellon, “Cardioprotective growth factors,” *Cardiovasc Research*, vol. 83, pp. 179–194, 2009.

[59] Z. Tao, B. Chen, X. Tan, Y. Zhao, L. Wang, T. Zhu, K. Cao, Z. Yang, Y. W. Kan, and H. Su, “Coexpression of VEGF and angiopoietin-1 promotes angiogenesis and cardiomyocyte proliferation reduces apoptosis in porcine myocardial infarction (MI) heart.,” *PNAS*, vol. 108, no. 5, pp. 2064–9, Feb. 2011.

[60] S. Taghavi and J. C. George, “Homing of stem cells to ischemic myocardium,” *J Transl Res*, vol. 5, no. 4, pp. 404–411, 2013.

[61] C. Zhu, X. Qi, Y. Chen, B. Sun, Y. Dai, and Y. Gu, “PI3K/Akt and MAPK/ERK1/2 signaling pathways are involved in IGF-1-induced VEGF-C upregulation in breast cancer.,” *Journal of cancer research and clinical oncology*, vol. 137, no. 11, pp. 1587–94, Nov. 2011.

[62] R. Qiu, A. Cai, Y. Dong, Y. Zhou, D. Yu, Y. Huang, and D. Zheng, “SDF-1 α upregulation by atorvastatin in rats with acute myocardial infarction via nitric oxide production confers anti-inflammatory and anti-apoptotic effects,” *Journal of Biomedical Science*, vol. 19, no. 99, 2012.

[63] S. Sukhanov, Y. Higashi, S.-Y. Shai, C. Vaughn, J. Mohler, Y. Li, Y.-H. Song, J. Titterington, and P. Delafontaine, “IGF-1 reduces inflammatory responses, suppresses oxidative stress, and decreases atherosclerosis progression in ApoE-deficient mice.,” *Arteriosclerosis, thrombosis, and vascular biology*, vol. 27, no. 12, pp. 2684–90, Dec. 2007.

[64] I. Beberashvili, I. Sinuani, A. Azar, H. Kadoshi, G. Shapiro, L. Feldman, and J. Sandbank, “Decreased IGF-1 levels potentiate association of inflammation with all-cause and cardiovascular mortality in prevalent hemodialysis patients .,” *Growth Horm IGF Res.*, vol. 23, no. 6, pp. 209–214, 2013.

[65] S. K. Gupta, K. Pillarisetti, and P. G. Lysko, “Modulation of CXCR4 expression and SDF-1 α functional activity during differentiation of human monocytes and macrophages Abstract : Chemoattraction of monocytes by the the regulation of CXCR4 transcription and SDF-1- mRNA in HL-60 cells and does not cause,” *Journal of Leukocyte Biology*, vol. 66, pp. 135–143, 1999.

[66] Y.-X. Sun, J. Wang, C. E. Shelburne, D. E. Lopatin, A. M. Chinnaiyan, M. a Rubin, K. J. Pienta, and R. S. Taichman, “Expression of CXCR4 and CXCL12 (SDF-1) in human prostate cancers (PCa) in vivo.,” *Journal of cellular biochemistry*, vol. 89, no. 3, pp. 462–73, Jun. 2003.

[67] M. S. Penn, “Importance of the SDF-1:CXCR4 axis in myocardial repair.,” *Circulation research*, vol. 104, no. 10, pp. 1133–5, May 2009.

[68] A. Mathiasen, M. Haack-Sørensen, J. E, and K. J., “Autotransplantation of mesenchymal stromal cells from bone-marrow to heart in patients with severe stable coronary artery disease and refractory angina--final 3-year follow-up,” *Int J Cardiol.*, vol. 170, no. 2, pp. 246–251, 2013.

[69] M. R. Duranski, J. J. M. Greer, A. Dejam, S. Jaganmohan, N. Hogg, W. Langston, R. P. Patel, S. Yet, X. Wang, C. G. Kevil, M. T. Gladwin, and D. J. Lefer, “Cytoprotective effects of nitrite during in vivo ischemia-reperfusion of the heart and liver,” *Journal of Clinical Investigations*, vol. 115, no. 5, 2005.

[70] F. M. Gonzalez, S. Shiva, P. S. Vincent, L. A. Ringwood, L. Hsu, Y. Y. Hon, A. H. Aletras, O. Richard, C. Iii, M. T. Gladwin, and A. E. Arai, “Nitrite Anion (NO2−) Provides Potent Cytoprotective and Antiapoptotic Effects as Adjunctive Therapy to Reperfusion for Acute Myocardial Infarction,” *Circulation*, vol. 117, no. 23, pp. 2986–2994, 2008.

[71] R. Schulz, M. Kelm, and G. Heusch, “Nitric oxide in myocardial ischemia / reperfusion injury,” *Cardiovascular Research*, vol. 61, pp. 402–413, 2004.

[72] N. Neye, F. Enigk, H. Habazettl, N. Plesnila, H. Kuppe, M. T. Gladwin, and W. M. Kuebler, “Inhalation of NO during myocardial ischemia reduces infarct size and improves cardiac function,” *Intensive Care Med*, vol. 38, pp. 1381–1391, 2012.

[73] F. Brunner, R. Maier, P. Andrew, G. Wölkart, R. Zechner, and B. Mayer, “Attenuation of myocardial ischemia/reperfusion injury in mice with myocyte-specific overexpression of endothelial nitric oxide synthase.,” *Cardiovascular research*, vol. 57, no. 1, pp. 55–62, Jan. 2003.

[74] Z. Liu, H. Wang, Y. Wang, Q. Lin, A. Yao, F. Cao, D. Li, J. Zhou, C. Duan, Z. Du, Y. Wang, and C. Wang, “Biomaterials The in fl uence of chitosan hydrogel on stem cell engraftment , survival and homing in the ischemic myocardial microenvironment,” *Biomaterials*, vol. 33, no. 11, pp. 3093–3106, 2012.

7. Abbreviations

BAD	Bcl-2-Antagonist of cell death
BM	basement membrane
BMSC	bone marrow derived stem cells
cAMP	cyclic adenosine monophosphate
CD	cluster of differentiation
cGMP	cyclic guanosine monophosphate
Cq	quantification cycle
Ct	threshold cycle
CXCL-12	chemokine (C-X-C motif) ligand 12
CXCR-4	chemokine (C-X-C motif) receptor 4
DMSO	dimethyl sulfoxide
dNTP	deoxyribonucleotidetriphosphate
EC	endothelial cells
ECM	extra cellular matrix
eNOS	endothelial nitric oxide synthase
EPO	erythropoietin
ERK	extracellular-signal regulated kinases
ETS-1	E26 transformation-specific –transcription factor 1
FAK	focal adhesion kinase
FBS	fetal bovine serum
FGF	fibroblast growth factor
FKHR	forkhead in rhabdomyosarcoma
GAPDH	glyceraldehyde 3-phosphate dehydrogenase
HBTU	O-Benzotriazole-N,N,N’,N’-tetramethyl-uronium-hexafluoro-phosphate
HE	hematoxylin and eosin
HIF-1α	hypoxia-inducible factor 1-alpha
HLA-DR	human leukocyte antigen DR
HPLC	high-performance liquid chromatography

HSF-1	heat Shock Factor 1
IGF-1	insulin like growth factor -1
IGFBP	insulin like growth factor binding protein
IGF-R	insulin like growth factor receptor
IL-6	Interleukin 6
IR	insulin receptor
LC-MS	liquid chromatography–mass spectrometry
MAPK	mitogen-activated protein kinase
MCP-1	monocyte chemotactic protein-1
MDM-2	mouse double minute 2 / E3 ubiquitin-protein ligase
MEK 1/2	mitogen activated protein kinase
MMP	matrix metalloproteinases
MSC	mesenchymal stem / stroma cells
NF-kappa	nuclear factor *kappa*-light-chain-enhancer
NO	nitric oxide
NOS	nitric oxide synthase
P/S	penicillin / streptomycin
$p/s/cm^2/sr$	photons per second per centimeter squared per steradian
PDGF	platelet-derived growth factor
PI3K	phosphoinositide 3-kinase
PKC	protein kinase C
PLC-γ	phospholipase C-γ
RISK	reperfusion injury salvage kinase
ROS	reactive oxygen species
SDF-1	stromal cell-derived factor 1
TGF-ß	transforming Growth Factor beta
TNF-α	tumour necrosis factor-alpha
VEGF	vascular endothelial growth factor
VEGF-R	vascular endothelial growth factor receptor

8. Index of Figures

Fig.1: Process of angiogenesis in ischemic tissue [12]. For description see text. -6-

Fig.2: PKA signaling modulates the effects of NO in vascularization. PKA-dependent signaling pathway is activated by stimuli such as mechanical forces and chemical ligands which are regulating vessel growth. The PKA pathway interacts with several intracellular pathways (PI3K, Akt and AMPK) to activate eNOS/NO. eNOS/NO induces multiple cellular functions (cell proliferation, migration and survival) leading to angiogenesis and ischemic vessel growth [1]. -9-

Fig.3: IGF-1 mediated signaling results in regulation of cell growth and proliferation, cell survival and motility, and invasion. Green lines show activation whereas red lines depict inhibition. The signaling downstream of IGF1R, insulin receptor (IR) and hybrid receptors, and their principal effectors is pictured. After IGF1R activation, regulatory (p85) and catalytic (p110) subunits of PI3K are recruited. PIP3 production activates PDK-1, which activates AKT. AKT is also activated by the mTORC2 complex, initiated by an unknown mechanism by the IGF1R. AKT promotes cell survival, stabilizes the mitochondrial membrane, inhibits apoptosis, induces the expression of pro-survival genes and blocks the expression and function of growth inhibitors. The mTORC1 complex enhances the translation of proteins involved in proliferation. Activation of RAS, RAF and mitogen-activated protein kinase isoforms ERKs, p38 and JNK, results in transcription of proliferative genes. Motility and migration are enhanced by cross-talk between the IGF1R and integrins, leading to actin reorganization and actin/myosin contractility. IGFs induce the expression of MMPs, for invasion and stimulate angiogenesis by activating endothelial nitric oxide synthase and induce expression of hypoxia-inducible factor-1a and vascular endothelial growth factor [41]. -12-

Fig.4: Structure of the active site of the IGF-1 protein linked to the gel forming compound NapFFG. -17-

Fig.5: Temperature schema for qPCR -23-

Fig.6: LC-MS analysis of the NapFFG-IGF-1 active site hydrogel powder. The NapFFG-IGF-1 active site hydrogel was separated on a reverse phase HPLC and the eluent monitored at 220nm and 254nm (A). The mass spectrumof the eluent at ~3.5 min is depicted in (B). -30-

Fig.7: Effect of NapFFG-NO and NapFFG-IGF on the proliferation of MSC. MSC were incubated with MEM-α-medium, medium containing NapFFG, NapFFG-NO or NapFFG-IGF-1. After 24h, 48h and 72h the MTT reagent was added, and the absorbance of the reduced MTT tetrazole determined at 490nm. Data are mean + SD (n=4, *** p <0.001, ** p <0.01, * p <0.05). -31-

Fig.8: Relative mRNA expression level of VEGF in MSC. VEGF mRNA expression levels were determined by qRT-PCR in MSC cultured for 24h in MEM-α-medium (MSC only = control), medium containing NapFFG-NO, NapFFG-IGF-1 or NapFFG. Incubations were performed under standard ("normal") conditions and under ischemic conditions as mimicked by the presence of H_2O_2. Relative expression levels of VEGF were calculated using the quantification cycle (Cq), that represents the number of cycles necessary to reach a threshold signal level and were normalized to GAPDH expression level. Data are mean + SD (n=3, *** p <0.001, ** p <0.01, * p <0.05). -33-

Fig.9: VEGF mRNA expression level in MSC upon treatment. VEGF mRNA expression levels were determined by qRT-PCR in MSC cultured for 24h in MEM-α-medium (MSC only = control), medium containing NapFFG-IGF-1, NapFFG-NO, or NapFFG, under "normal" (standard cell culture) as well as under ischemic conditions as mimicked by the presence of H_2O_2. The ddCt was calculated using GAPDH expression as a control and the ratio between of untreated and treated cells termed as "normal" and ischemic conditions was calculated. Data are mean + SD (n=3, ** p <0.01). -34-

Fig.10: Relative expression level of SDF-1 in MSC. SDF-1 mRNA expression levels were determined by qRT-PCR in MSC cultured for 24h in MEM-α-medium control, medium containing NapFFG-IGF-1, NapFFG-NO or NapFFG under "normal" (standard cell culture) as well as under ischemic conditions as mimicked by the presence of H_2O_2. Relative expression levels of SDF-1 were calculated using the quantification cycle (Cq) that represents the number of cycles necessary to reach a threshold signal level and were normalized to GAPDH expression level. Data are mean + SD (n=3, *** p <0.001, ** p <0.01, * p <0.05). -35-

Fig.11: SDF-1 mRNA expression level in MSC upon treatment. SDF-1 mRNA expression levels were determined by qRT-PCR in MSC cultured for 24h in MEM-α-medium(MSC only), medium containing NapFFG-IGF-1, NapFFG-NO or NapFFG, under normal (standard cell culture) as well as under ischemic conditions as mimicked with H_2O_2. The ddCt was calculated using GAPDH expression as a control and the ratio between of untreated and treated cells termed as "normal" and ischemic conditions was calculated. Data are mean + SD (n=3, * p <0.05). -37-

Fig.12: Luminescence signal of MSC in C57 mice. The luminescence signal was detected at day 1, 3, 5 and 7 after infarction and injection of MSC in media (MSC only), MSC in NapFFG-hydrogel and MSC in NO-releasing hydrogel. Mice received an injection of the substrate and the luminescence signal was detected during a 5min exposure time. -38-

Fig.13: Luminescence signal of MSC in FVB mice. The luminescence signal was detected at day 1, 3, 5 and 7 after infarction and injection of MSC in media (MSC only), MSC in NapFFG-hydrogel and MSC in NO-releasing hydrogel. Mice received an injection of the substrate and the luminescence signal was detected during a 5min exposure time. -39-

Fig.14: Luminescence signal of MSC in mice. The luminescence signal was detected by molecular imaging at day 1, 3, 5 and 7 after infarction and injection of MSC in media (MSC only), MSC in NapFFG-hydrogel and MSC in NO-releasing hydrogel in the infarcted heart. The figure shows the average of photons per second per square centimeter per steradian after 5min exposure time. Data are mean + SD (n=5, *** p <0.001, ** p <0.01, - p >0.05). -41-

Fig. 15: Cross-sections of HE and Masson's Trichrome stained hearts. Mice were sacrificed 1 week after infarction and injection of MSC in saline (MSC only), MSC in NapFFG-hydrogel or MSC in NO-releasing hydrogel. Then, tissue sections were HE and Masson's Trichrome stained and pictures taken at 2,5x magnification. -42-

Fig. 16: Percentage of the infarcted area in the left ventricle after seven days of myocardial infarction. The infarct size was calculated by the size of the collagen area compared to the size of the left ventricle using stained hearts of mice, sacrificed 7 days after permanent ligation of the left descending coronary artery and injection of MSC in saline (MSC only = control), NapFFG-hydrogel or a NO-releasing hydrogel. Data are mean + SD (n=5, * p <0.05). -43-

Fig. 17: Cross-sections of HE and Masson's Trichrome stained hearts. Mice were sacrificed 1 month after infarction and injection of MSC in saline (MSC only), MSC in NapFFG-hydrogel or MSC in NO-releasing hydrogel. Then, tissue sections were HE and Masson's Trichrome stained and pictures taken at 2,5x magnification. -44-

Fig. 18: Percentage of the infarcted area in the left ventricle one month after myocardial infarction. The infarct size was calculated by the size of the collagen area compared to the size of the left ventricle using stained hearts of mice, sacrificed 1 month after permanent ligation of the left descending -45-

coronary artery and which had received either injections of MSC in saline (MSC only control) or in a NO-releasing hydrogel. Data are mean + SD (n=5, *** p <0.001).

Fig. 19: Percentage of the infarcted area in the left ventricle one week and one month after myocardial infarction. The infarct size was calculated using the stained hearts of mice, sacrificed one week and one month after permanent ligation of the left descending coronary artery and injection of MSC in saline (MSC only =control) or in a NO-releasing hydrogel. Data are mean + SD (n=5, ** p <0.01, - p >0.05). -46-

9. Index of Tables

Tab.1: Eluation-program for LC-MS mass detection -18-

Tab.2: Eluation-program for the purification using HPLC -19-

Tab.3: Primers used for RT-PCR -23-

10. Acknowledgements

At this juncture I would like to thank everybody, who accompanied and supported me during my academic studies and this thesis.

First of all I would like to thank my supervisors Prof. Achim Lass and Dr. Dagmar Pfeiffer for the great supervision. Especially I would like to thank Dr- Pfeiffer for the opportunity to go to China and for her boundless encouragement over the continents.

Secondly I would also like to thank Prof. Deling Kong for the chance to perform my work in his lab. In this connection the financial support of the European Union within the project "**EU-FP7: ABREM** - Advanced Biomaterials for Regenerative Medicine" has to be appreciated.

In China especially Yao XinPeng's help with the experiments and particularly his help with the language problem in the lab and elsewhere is highly acknowledged. In this connection I would also like to thank Zhihong Wang and Wenting Zheng. Not only their help, but also the enrichment of any cultural aspects I got is highly cherished. Furthermore Dr. Liu Yi's work regarding the animal experiments is highly appreciated.

At the end I would like to thank my family; especially my father and my sister for their love and support at any given moment during my academic studies and my adventurous life in China. Without their relief many obstacles could not have been overcome that easily. Additionally I would like to thank for their endurance, understanding and patience with me and my plans at home and abroad.

11. Declaration

Ich erkläre an Eides statt, dass ich die vorliegende Arbeit selbstständig verfasst, andere als die angegebenen Quellen/Hilfsmittel nicht benutzt, und die den benutzten Quellen wörtlich und inhaltlich entnommenen Stellen als solche kenntlich gemacht habe. Das in TUGRAZonline hochgeladene Textdokument ist mit der vorliegenden Masterarbeit identisch.

I declare that I have authored this thesis independently, that I have not used other than the declared sources/resources, and that I have explicitly indicated all material which has been quoted either literally or by content from the sources used. The text document uploaded to TUGRAZonline is identical to the present master‘s thesis.

Date Christina Stefanitsch